

## General Disclaimer

### One or more of the Following Statements may affect this Document

- This document has been reproduced from the best copy furnished by the organizational source. It is being released in the interest of making available as much information as possible.
- This document may contain data, which exceeds the sheet parameters. It was furnished in this condition by the organizational source and is the best copy available.
- This document may contain tone-on-tone or color graphs, charts and/or pictures, which have been reproduced in black and white.
- This document is paginated as submitted by the original source.
- Portions of this document are not fully legible due to the historical nature of some of the material. However, it is the best reproduction available from the original submission.

**NASA TECHNICAL  
MEMORANDUM**

**NASA TM X-73,183**

**NASA TM X-73,183**

**(NASA-TM-X-73183) FURTHER STUDIES OF STATIC  
TO FLIGHT EFFECTS ON FAN TONE NOISE USING  
INLET DISTORTION CONTROL FOR SOURCE  
IDENTIFICATION (NASA) 42 p HC A03/MF A01**

**N77-14027**

**Unclas**

**CSCL 20A G3/07 58295**

**FURTHER STUDIES OF STATIC TO FLIGHT EFFECTS ON FAN TONE NOISE  
USING INLET DISTORTION CONTROL FOR SOURCE IDENTIFICATION**

**Brent K. Hodder**

**Ames Research Center, NASA  
and  
Ames Directorate, USAAMRDL  
Ames Research Center, Moffett Field, CA 94035**

**December 1976**



1. Report No. NASA TM X-73,183	2. Government Accession No.	3. Recipient's Catalog No.	
4. Title and Subtitle FURTHER STUDIES OF STATIC TO FLIGHT EFFECTS ON FAN TONE NOISE USING INLET DISTORTION CONTROL FOR SOURCE IDENTIFICATION		5. Report Date	
		6. Performing Organization Code	
7. Author(s) Brent K. Hodder		8. Performing Organization Report No. A-6821	
		10. Work Unit No. 505-03-12	
9. Performing Organization Name and Address Ames Research Center and U.S. Army Air Mobility R&D Laboratory Moffett Field, Calif. 94035		11. Contract or Grant No.	
		13. Type of Report and Period Covered Technical Memorandum	
12. Sponsoring Agency Name and Address NASA, Washington, DC 20546 and US Army Air Mobility R&D Laboratory Moffett Field, CA 94035		14. Sponsoring Agency Code	
		15. Supplementary Notes	
16. Abstract  <p>Current experimental investigations have linked static inflow distortion phenomena such as the ground vortex, atmospheric turbulence, and test-stand structure interference to the generation of fan tone noise at the blade passing frequency. Since such distortions do not exist in flight, it is important to remove them from the static test environment and thereby improve the static-to-flight tone-noise correlation. In the course of providing evidence for this position, a recent investigation used a distortion control inlet with a modern day turbofan engine to assess atmospheric turbulence effects. Although the initial results were encouraging, they were incomplete. The present investigation continues this work and shows more completely the effect of atmospheric turbulence on tone-noise generation. Further, use is made of the distortion control inlet to identify other competing tone-noise sources in the test engine such as a rotor-core stator interaction which was confirmed by engine modifications.</p>			
17. Key Words (Suggested by Author(s)) Aeroacoustics Fan noise reduction		18. Distribution Statement Unlimited  STAR Category - 07	
19. Security Classif. (of this report) Unclassified	20. Security Classif. (of this page) Unclassified	21. No. of Pages 42	22. Price* \$3.75

## SYMBOLS

B	number of rotor blades
$f_1$	fundamental harmonic of the fan blade passing frequency
h/D	ratio of engine centerline height above ground to engine fan diameter
$K'_{m\mu\sigma}$	characteristic wave number
$\ell/d$	ratio of honeycomb cell axial length to cell diameter
$M_m$	circumferential Mach number for m lobe pattern, $\frac{BM_r}{m}$
$M_m^*$	cutoff Mach number, $\frac{K'_{m\mu\sigma}}{m}$
$M_r$	rotor Mach number at desired fan radius
m	lobe number
$P_T/P_{T_0}$	ratio of fan bypass exhaust total pressure to ambient total pressure
r/R	ratio of local bypass exhaust nozzle radius to maximum bypass exhaust nozzle radius
rpm <sub>c</sub>	fan rotational speed corrected to standard-day
SPL	sound pressure level, dB ref 0.0002 $\mu$ bar
T	engine total thrust, N
$T_1$	engine inlet temperature, °F
$\theta$	angle of far-field microphone relative to engine rotational axis, deg
$\phi$	circumferential position of in-duct microphone, deg
$\xi_m$	cutoff ratio, $M_m/M_m^*$
$\mu$	radial mode index
$\sigma$	fan rotor hub-tip ratio
$\delta$	relative static pressure

# FURTHER STUDIES OF STATIC TO FLIGHT EFFECTS ON

## FAN TONE NOISE USING INLET DISTORTION

### CONTROL FOR SOURCE IDENTIFICATION

Brent K. Hodder

Ames Research Center

and

U.S. Army Air Mobility R&D Laboratory

#### SUMMARY

An experimental investigation reported in reference 1 linked inflow distortion phenomena such as ground vortex, atmospheric turbulence, and test-stand structure interference to the generation of fan tone noise at the blade passing frequency. Since such distortions do not exist in flight, the results in reference 1 emphasized the need to remove them from the static test environment and thereby improve the static-to-flight tone-noise correlation. However, it was concluded from the results in reference 1 that the total effect of these distortion phenomena and particularly that of atmospheric turbulence had not been found. This problem was thought to be caused by a competing tone-noise level radiated from a rotor-core stator interaction and an inlet temperature probe-rotor interaction occurring in the test engine. In this investigation, both the core stator and the inlet temperature probe were modified to ascertain their contribution to the generation of tone noise at the blade passing frequency.

Experimental results have confirmed that both the rotor-core stator and the temperature probe-rotor interactions did generate sufficient sound pressure levels at the blade passing frequency to obscure turbulence-related tone noise on and near the fan axis. Atmospheric turbulence effects were reexamined with the modified engine and the distortion control inlet used in reference 1. Results showed a large reduction in both the level and variability of noise radiated at the blade passing frequency. Reductions in far-field, sound-pressure levels of 7 dB were measured from an on-axis location up to 60° off-axis. Because the test procedures used here were like those in reference 1, a more isolated assessment of atmospheric turbulence effects was possible. The reductions achieved using the distortion control inlet indicate the importance of removing atmospheric turbulence effects.

Of equal importance was the clear identification of rotor-core stator interaction tones in the test engine whose design is similar to other current low-noise, high-bypass turbofan engines. The results indicate that this source of tone noise should not be ignored in the design of future low-noise engines.

## INTRODUCTION

Currently, the prediction of inflight aircraft propulsion noise is based on static measurements extrapolated to flight conditions. One area where this approach has not proved successful is in the prediction of fan noise at the fundamental blade passing frequency from modern turbofan engines. Flight measurements have been shown to be from 5-10 dB lower than predicted from static measurements.

In an effort to improve static prediction of flight tone-noise levels, reference 1 focused attention on the importance of controlling engine inflow distortions common to conventional static test environments. The test engine used in reference 1, a production Pratt and Whitney JT15D-1 turbofan, had been shown (ref. 2) to exhibit lower inflight sound pressure levels at the blade passing frequency. Engine inflow distortions investigated in reference 1, like the ground vortex, atmospheric turbulence, and test-stand structure interference, were shown to substantially increase the sound pressure levels and variability of noise at the blade passing frequency. Since these distortion phenomena do not exist in flight, they obviously prevent accurate static predictions of inflight levels.

During the investigation of atmospheric turbulence effects in reference 1, test results were interpreted to indicate that a strong rotor-stator interaction source remained in the test engine. In effect, this interaction was thought to be obscuring some of the benefits predicted from small-scale data of using a distortion control inlet to destroy rotor-inflow turbulence interactions. The opportunity for rotor-stator radiation existed in the test engine due to the particular design of the fan outlet guide vane stator. A split vane stator assembly was used in which the vane/blade ratio for cutoff and spacing are provided only in the outer vane segment for bypass flow. The inner stator segment for core flow was not designed for cutoff and only aerodynamic spacing was used. Although the cut-on condition of the core stators was recognized before the investigation in reference 1, it was considered impossible to accurately predict its radiated levels.

To confirm that the rotor-core stator interaction was generating sufficient tone levels to obscure some of the benefits of a distortion control inlet, a follow-on experimental investigation was conducted. In addition to the core stator interaction, the effect of the presence of an inlet temperature-sensing probe in the production engine, which protrudes from the inlet duct outer wall in front of the fan rotor, was investigated. This report presents the results from this investigation.

## TEST APPARATUS

A production Pratt and Whitney JT15D-1 turbofan engine was used for this investigation. The JT15D-1 incorporates many of the established design techniques for reduced engine noise (see table I). The outdoor static test

facility is shown in figure 1. The test facility and engine mounting arrangement were somewhat different from that used in reference 1 because of the necessity to piggyback this program onto a following wind-tunnel investigation. Therefore, the static installation used reflects the wind-tunnel mounting arrangement. However, this mounting system still maintained in large engine-ground clearance and "cleanness" of installation like that used in reference 1 to investigate atmospheric turbulence effects. The engine was top-mounted to a pylon attached to a 3.048-m span wing. The engine centerline was 7.7 fan diameters above the ground, and the bellmouth inlet was cantilevered 5.1 fan diameters forward of the test-stand-support struts (fig. 2).

The same distortion control bellmouth inlet used in reference 1 was used for this investigation and is shown in figures 3 and 4. The inlet design provides for the installation of a honeycomb matrix across the inlet duct to destroy inflow distortions. The design procedure used for this particular inlet is discussed in reference 1. The inlet duct consisted of a conventional bellmouth inlet, a spacer section (with or without the honeycomb matrix), a constant-diameter section, and, finally, a contraction section leading to the rotor inlet plane. A duct area ratio of 2.5 was provided between the location of the honeycomb matrix and the fan rotor annulus. This allowed lower inlet velocities through the honeycomb and subsequently low inlet total pressure losses.

For the investigation of the core stator contribution to tone noise, both a production stator and a modified production stator were used. The production stator assembly (fig. 5) contains 66 vanes in the outer section for bypass flow and 33 vanes in the inner section for core flow. In the modified stator assembly (fig. 6), the inner-core vane section was removed and replaced by outer- and inner-flow path liners to maintain the original flow-path contours. It was felt that removing the core stators was the best overall method to assess their tone noise contribution even though some aerodynamic penalties would be incurred. An alternate method of increasing rotor-stator spacing was ruled out due to the inability to substantially increase spacing without extensive modifications to the core stator vanes. In contrast, removing the core stator assembly involved only a simple mechanical attachment. Predicted engine performance with the core stators removed was supplied by the engine manufacturer. The performance analysis concluded that, with the core stators removed, six engine casing struts downstream of the core stator position could be used to obtain all of the necessary flow turning. This approach would cause an increase in total pressure loss, but the losses were expected to remain within acceptable limits. The ability to obtain greater flow turning with only six struts stemmed mainly from their large chord and resultant high solidity of 0.75 at the hub and 1.2 at the tip. Fortunately, the casing struts were sufficiently far downstream of the rotor, 2.49 local projected rotor chords, that they did not generate strong interaction tones themselves. Hence, it was concluded that a meaningful exploratory noise test could be made with the core stators removed.

The other engine modification performed for this investigation involved the inlet temperature sensing ( $T_1$ ) probe shown in figure 7. This airfoil-shaped probe is mounted approximately 1 probe chord in front of the fan rotor

and 20° off the vertical centerline of the fan. The presence of the production  $T_1$  probe causes rotor-blade lift fluctuations that result in tone noise generation. These lift fluctuations are caused by the following: first, the wake from the probe body itself creates a velocity nonuniformity the rotor blades pass through which is analogous to a stator-rotor interaction. Further, and perhaps more importantly, another velocity nonuniformity is created by the discharge of compressor bleed air from the probe at two locations shown in figure 7. The discharge of compressor bleed air results from its use for probe leading-edge anti-icing and for a jet pump to force ambient air over the thermocouple sensors. The total jet pump flow (spilled air) is then discharged at the base of the probe (fig. 7).

The production  $T_1$  probe installation (fig. 8) was modified by first moving the probe body radially outward in its mount so that only the thermocouple junction protruded into the inlet duct (fig. 9). This was accomplished by simply using a spacer block in the normal probe-mounting boss on the outside of the engine inlet duct. The probe airfoil-shaped body was then potted with flexible epoxy to fill up the cavity left between the probe body and a circular hole in the duct wall originally occupied by the probe base. Finally, the compressor bleed air lines to the probe assembly were capped off as was the bleed intake orifice in the probe assembly. This modification was also coordinated with the engine manufacture to ensure that inlet temperature would not be grossly affected and thereby jeopardize its function in engine operation. Figure 10 is a summary schematic of the modified engine versus a production JT15D-1 engine.

Finally, figure 11 shows the installation of the JT15D-1 in the 40- by 80-Foot Wind Tunnel. A cruise inlet (described in ref. 1) is shown installed on the engine.

#### DATA ACQUISITION AND PROCEDURES

Static far-field acoustic data were measured with an array of 1.27-cm-diameter condenser microphones placed on a 15.24 m radius from the fan inlet (fig. 12). The microphones were positioned in the plane of the engine horizontal centerline. Acoustic measurements were also made in the fan inlet duct both statically and in the wind tunnel at three different circumferential positions forward of the fan rotor (fig. 13). Measurements were made using 0.254-cm-diameter piezoelectric microphones flush-mounted in the inlet duct wall. All static far-field and in-duct acoustic measurements were taken simultaneously to allow a direct comparison. In addition, both far-field and in-duct microphone positions relative to the engine were identical to those in reference 1.

Acoustic data were FM recorded on magnetic tape at 30 ips with a frequency response from dc to 20 KHz. All data analyses were performed from tape recorded data. Spectrum analysis was performed with a narrowband real-time spectrum analyzer with integrating capability. The spectrum analyzer resolution bandwidth was 25 Hz, which equates to a noise bandwidth of 47 Hz.

No corrections for ground reflections or atmospheric absorption were applied to the data presented.

Engine thrust measurements were obtained using the force balance system in the 40- by 80-Foot Wind Tunnel.

## RESULTS AND DISCUSSION

Reference 1 suggested, based on measured results, that the total effectiveness of a distortion control inlet may not have been ascertained because of the dominance, in the test engine, of tone noise sources not related to inflow distortions. Candidate sources of this type in the test engine were thought to be the cut-on rotor-core stator and  $T_1$  probe-rotor interactions. The purpose of this investigation was to assess the magnitude of these interaction sources and, if warranted, reexamine the effectiveness of the distortion control inlet without their presence.

To put the problem into perspective, figures 13 and 14 from reference 1 are presented as figures 14 and 15 in this report to review the initial results that placed suspicion on the rotor-core stator interaction and the  $T_1$  probe-rotor interaction. The results from reference 1 indicated that, while there was a large reduction of  $f_1$  SPL variability with installation of the honeycomb matrix, there was little definitive reduction in average far-field and in-duct  $f_1$  SPL (contrary to small-scale results). The  $f_1$  variability trends were reexamined in reference 1 by means of the probability density function. These results are presented again in figure 16. With turbulence control (honeycomb in), the probability density function changed from a more Gaussian distribution to one with the characteristic dip indicative of both random and sinusoidal behavior. As discussed in reference 1, sinusoidal behavior is more relatable to a rotor-stator-type interaction. Thus, the results were thought to indicate that, while distortion control (honeycomb in) reduced the turbulence-rotor source, a rotor-stator-type source of similar strength remained, which caused little difference in average  $f_1$  levels both in the far field and in the duct. The reduction in  $f_1$  variability was detectable due to the much greater sound pressure level excursions about the mean with the atmospheric turbulence-rotor source than with the rotor-stator-type source. The most obvious sources of interaction tones in the test engine were those resulting from the rotor-core stator and  $T_1$  probe-rotor interactions.

### Static Acoustic Results

To help isolate the core stator contribution, all measurements were made with the honeycomb matrix installed in the distortion control inlet and at an  $h/D = 7.7$ . This arrangement tends to remove a variety of other inflow distortion contributions to  $f_1$  SPL. Further, the  $T_1$  probe was modified (fig. 9) to eliminate its interaction with the rotor. With this test environment established, the contribution of the core stator was assessed by comparing

noise measurements with the core stator installed and removed. However, simply removing the core stator without some aerodynamic compensation would degrade rotor aerodynamics and thereby cloud the meaningfulness of the noise measurements. To guard against this, the decision to remove the core stator was predicated on the fact that, in this particular engine, six high-solidity casing struts farther downstream of the core stator, originally designed to supplement the core stators, would remain. Based on the engine manufacturers analysis, it was concluded that these casing struts could do all the required flow turning with an acceptable increase in total pressure loss and a decrease in core-mass-flow rates. Some concern was also expressed that the lower core-flow rates could degrade rotor performance in the bypass duct, starting with some instabilities at the entrance of the duct wall separating the core and bypass flow.

To avoid an exhaustive evaluation of engine aerodynamic performance with the core stators removed, it was felt that several easily measured engine parameters could be relied on to indicate acceptable engine operation. To assess flow conditions in the bypass duct, five four-element, total-pressure rakes were installed in the exhaust plane of the bypass duct. Only one of the five total pressure rake measurements (fig. 17) showed any meaningful loss in fan-pressure ratio with the core stator removed. However, even this loss would not be considered significant, and therefore no serious degradation in fan performance was indicated in the bypass flow as a result of removing the core stators. The extent of lower core flow and total pressure was evaluated by an overall engine thrust measurement and core operating exhaust gas temperature (EGT). Total thrust measurements were down only about 1 percent (fig. 18); starting and operating EGT's showed no difference from those EGT's encountered in production engine operation. With these results, it was felt that meaningful exploratory noise measurements could be made with the core stators removed.

First, the acoustic characteristics that would be expected from this particular rotor-core stator interaction should be established. The interaction of 28 rotor blades with 33 stator vanes produces a 5-lobe spinning pressure pattern. The cutoff ratio,  $\xi_m$ , at the approach power setting used (10,230 rpm) is 2.4 and therefore the 5-lobe mode will propagate.

The theoretical radiation pattern for this configuration predicts one major lobe that peaks in  $f_1$  SPL around 20-25° off the engine axis of rotation. Beyond approximately 35°, some additional lobe structure occurs but is at least 12 dB down from the peak level. The measured data with the core stator installed (fig. 19(a)) shows the peak level occurring on the axis with levels at 30° and beyond down a minimum of 14 dB. Although the theory would not predict on-axis radiation, there are some important similarities between theory and measured data. Both sets of data indicate peak levels occurring near the axis. Further, levels at 30° and beyond are at least 12 dB down from the peak levels. The fact that the measured data shows radiation on the axis may be a directivity effect caused by sound propagation through the honeycomb matrix.

As shown in figure 19(a), removal of the core stators reduced the strong on-axis radiation by 13 dB. Some reduction is also seen at angles other than 30°. Therefore, measured data have shown that core stator radiation behaved nominally as the theory would indicate and removal of the core stator essentially eliminated these characteristics. In-duct measurement (fig. 19(b)) also show reductions in  $f_1$  SPL from 3 to 6 dB (depending on duct microphone position) with the core stators removed.

To evaluate the  $T_1$  probe effects, noise measurements with the probe in the production engine position and in the modified position were compared. These data were obtained with the core stator removed and the distortion control inlet (honeycomb in) installed. The rotor inflow distortion produced by the production  $T_1$  probe can cause zeroth-mode propagation whose maximum levels are radiated on and near the axis. Accordingly, with the production  $T_1$  probe installed, the measured far-field data (fig. 20(a)) showed an increase of at least 6 dB in  $f_1$  SPL on the axis as well as 7 dB at 30°. Beyond 60°, the difference in  $f_1$  SPL generated by the two-probe configurations decreased rapidly. At  $\theta = 90^\circ$  and  $120^\circ$ , little significant difference in  $f_1$  SPL is shown. In-duct measurements (fig. 20(b)) proved more difficult to interpret. The modified  $T_1$  probe caused at least a 6-dB reduction in  $f_1$  SPL at the duct microphone nearest the  $T_1$  probe ( $\theta = 45^\circ$ ). The next closest microphone,  $\phi = 270^\circ$ , showed no change in  $f_1$  SPL with the  $T_1$  probe in either position. And, finally, the  $f_1$  SPL of the duct microphone most opposite the  $T_1$  probe location actually increased with the modified  $T_1$  probe installed from what is possibly a null point when the production  $T_1$  probe is installed.

From previous results, it seems clear that, because of the propagating modes involved and possible directivity effects caused by the honeycomb matrix, strong radiation from core rotor-stator interaction and  $T_1$  probe-rotor interaction occurred on and near the fan axis where turbulence-related tone noise would also be expected to radiate. The final piece of necessary evidence was to reassess atmospheric turbulence effects with the core stators removed and the modified  $T_1$  probe. Figure 21 presents data with the core stator and  $T_1$  probe modifications. Unlike the data in reference 1, reducing atmospheric turbulence distortions by installation of the honeycomb matrix now results in a decrease in average far-field  $f_1$  SPL of at least 7 dB from  $\theta = 0^\circ$  to  $60^\circ$  (see fig. 21(a)). All three in-duct microphones show (fig. 21(b)) a reduction in  $f_1$  SPL with the honeycomb matrix installed. Further, the in-duct measurement can also more accurately show the effect of turbulence control on  $f_1$  variability versus time. Figure 22 shows that distortion control (honeycomb in) reduced the peak-to-peak variability levels by at least 1/2, but the amount of variability with turbulence control is somewhat greater than was measured with the production engine in reference 1 because of the dominance of the more steady tones generated by the core stator and  $T_1$  probe interaction once the honeycomb matrix is installed. It is expected that the variability measured with the modified engine and distortion control could be improved simply by use of a slightly larger honeycomb matrix  $\ell/d$ . Trends to this effect were shown in reference 1 when  $\ell/d$  was increased from 8 to 10.

These data show more clearly than those in reference 1 the importance of removing atmospheric-turbulence-related phenomena from the static test environment and follow the predicted results based on the small-scale work in reference 4.

An interesting comparison can be made at this point of all contributors to on-axis  $f_1$  sound pressure levels. Figure 23 presents spectral analyses for each of the previous configurations investigated. Of primary interest is the fact that when all identified contributors, that is, core stators,  $T_1$  probe, and atmospheric turbulence, are removed, the resulting  $f_1$  SPL level is almost indistinguishable from the neighboring SPL's. Although the likelihood of this occurring once turbulence-related sources are removed has been discussed in the literature (ref. 5), this is the first time, to the author's knowledge, that measured data have come so close to predictions.

Another interesting comparison (fig. 24) is made between the current data and that measured in reference 1 with the production engine. Each curve in figure 24 for a particular configuration is a simple arithmetic average of the initial and repeat runs made for each configuration. Using the individual contributions from the rotor-core stator and  $T_1$  probe-rotor interactions, it seems possible to reconstruct the solid line that represents the production engine results from reference 1. The dominance of rotor-core stator contribution on-axis would appear to make it the prime source of on-axis levels in reference 1. At  $\theta = 30^\circ$ , the effects of  $T_1$  probe-rotor interaction seem to dominate and approximate the levels presented in reference 1. Beyond  $\theta = 30^\circ$ , the combined levels of both the rotor-core stator and  $T_1$  probe-rotor interactions would approach the reference 1 levels even if they were not totally in phase. Lastly, the modified and production engine (ref. 1)  $f_1$  SPL are compared, with both using turbulence control (honeycomb in), to demonstrate the dramatic effect of the engine modifications on the final  $f_1$  SPL results in each case, as well as any comparisons that might be made of forward arc sound power levels.

#### Wind-Tunnel Acoustic Results

A wind-tunnel test using the modified engine to investigate wind-tunnel simulation of in-flight fan noise characteristics followed the outdoor static test. Without digressing into the pros and cons of wind-tunnel simulation (which will be left to a later report), one can intuitively deduce that a wind tunnel, by its very nature, does not suffer from several of the inflow distortion problems associated with conventional outdoor static testing. Accordingly, the wind-tunnel program provided an opportunity to verify the core stator contribution with a more representative flight inlet in addition to the distortion control inlet.

The engine installation in the tunnel (shown in fig. 11) was essentially the same mounting arrangement as used in the static test. The flight inlet used is described in reference 1.

Of particular interest in the wind-tunnel measurement was the comparison of in-duct  $f_1$  SPL with the core stator in and out. These comparisons are presented in figure 25. The data were obtained with the modified  $T_1$  probe, a nominal tunnel velocity of 10.29 m/sec, and zero angle of attack. Like the static measurement made with the distortion control bellmouth inlet, all the cruise inlet duct microphones show a significant reduction in  $f_1$  SPL with the core stator removed. Since these measurements are made inside the inlet duct, they are not affected by tunnel reverberations.

#### CONCLUDING REMARKS

The supposition in reference 1 that atmospheric turbulence effects on tone noise generation were partially obscured by other competing tone noise sources in the test engine has been confirmed by this investigation. The competing tone noise sources were found to result from a fan rotor-core stator interaction and an inlet temperature probe-fan rotor interaction. These interaction sources were clearly identified by use of a distortion control inlet and by modifying the test engine so that it could be operated with and without the core stator and inlet temperature probe installed. The test engine, a Pratt and Whitney JT15D-1 turbofan, was the same as used in reference 1.

By operating the engine with the core stator removed and a modified inlet temperature probe, a more complete measurement of atmospheric turbulence effects was achieved. Installation of the distortion control inlet to reduce turbulence-related distortions (as anticipated in ref. 1) greatly reduced both the variability and the level of noise radiated at the blade passing frequency.

The fact that the rotor-core stator interaction produced substantial tone noise levels is in itself an important factor in establishing design criteria for low-noise engines. It has been common practice in the design of current low-noise turbofan engines to concentrate noise control features (vane/blade ratio and spacing) only on rotor-bypass stator interactions. However, the results of this investigation would indicate that rotor-core stator interaction noise must be more properly dealt with if further engine-noise reduction is to be achieved.

It seems reasonable to conclude that the results of this investigation have reinforced the arguments in reference 1 for the control of inflow distortions common to conventional static testing. Further, it is important to recognize that the identification of core stator radiation was really a by-product of achieving "cleaner" static test conditions more representative of flight environments.

## REFERENCES

1. Hodder, B. K.: An Investigation of Possible Causes for the Reduction of Fan Noise in Flight. AIAA Paper 76-585, July 1976.
2. Plucinsky, J. C.: Quiet Aspects of the Pratt and Whitney Aircraft JT15D Turbofan. SAE Paper 730,289, 1973.
3. Anon.: JT15D-1 Turbofan Engine Descriptive Notes. Part 3019440, United Aircraft of Canada, Ltd., May 1971.
4. Hodder, B. K.: Investigation of the Effect of Inlet Turbulence Length Scale on Fan Discrete Tone Noise. NASA TM X-62,300, 1973.
5. Rao, G. V. R.; Chu, W. T.; and Digumarthi, R. V.: Theoretical Studies of Tone Noise from a Fan Rotor. NASA CR-2354, Nov. 1973.

TABLE I.- PRODUCTION JT15D-1 FAN GEOMETRY AND ACOUSTIC DESIGN FEATURES

Single stage outlet guide vane fan (No IGVs)	—	
Bypass vane/blade ratio	2.36	
Core vane/blade ratio	1.18	
Rotor blades	28	
Bypass stator vanes	66	
Core stator vanes	33	
Bypass rotor - stator spacing	1.83	} Projected axial rotor chords
Core rotor - stator spacing	0.50	
Bypass ratio	3.3	
Fan pressure ratio	1.5	
Hub/tip ratio	0.405	
Maximum fan rpm	16000	
Rotor diameter	53.34 cm	

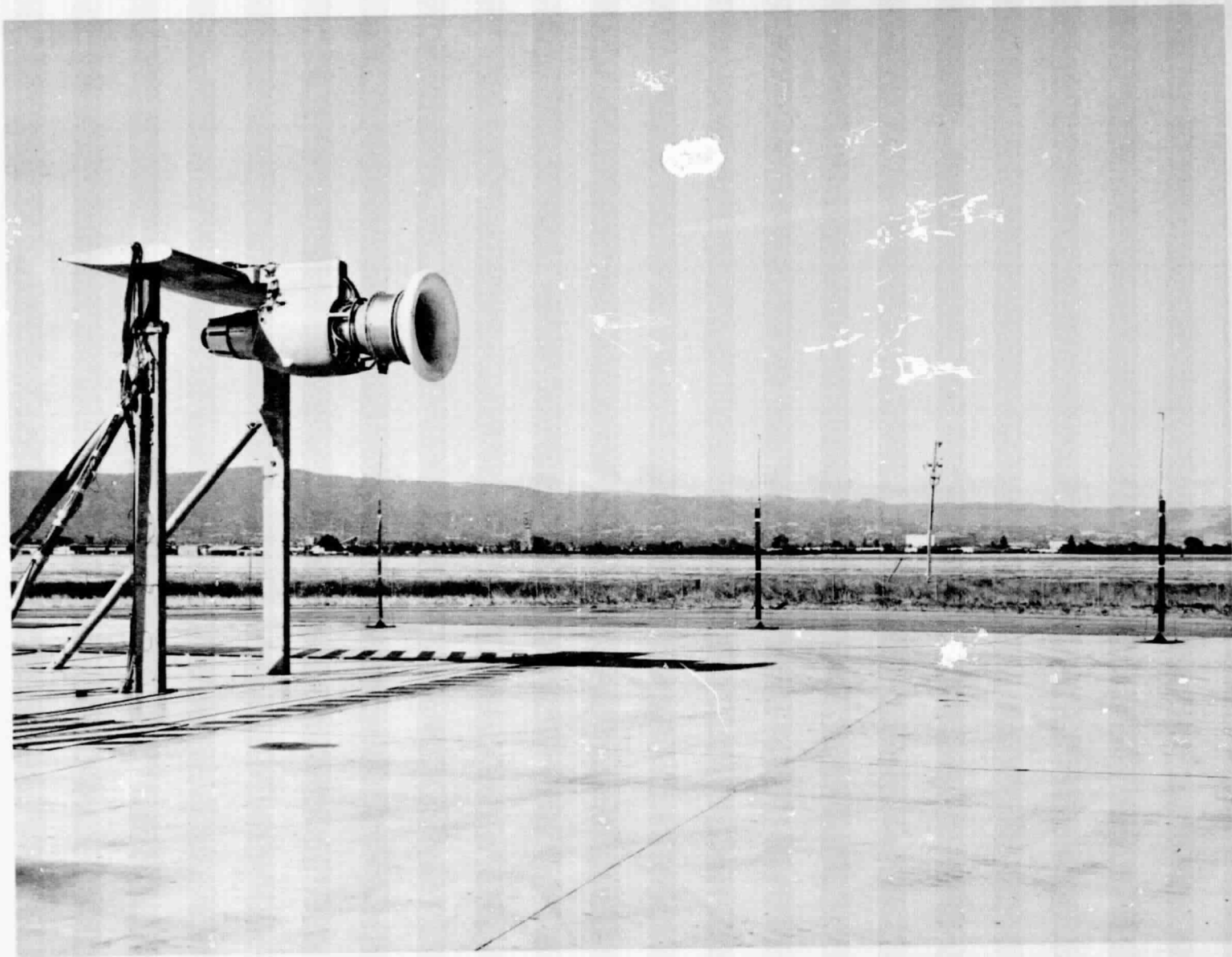


Figure 1.- Photograph of static test installation of JT15D-1 engine with distortion control bellmouth inlet.

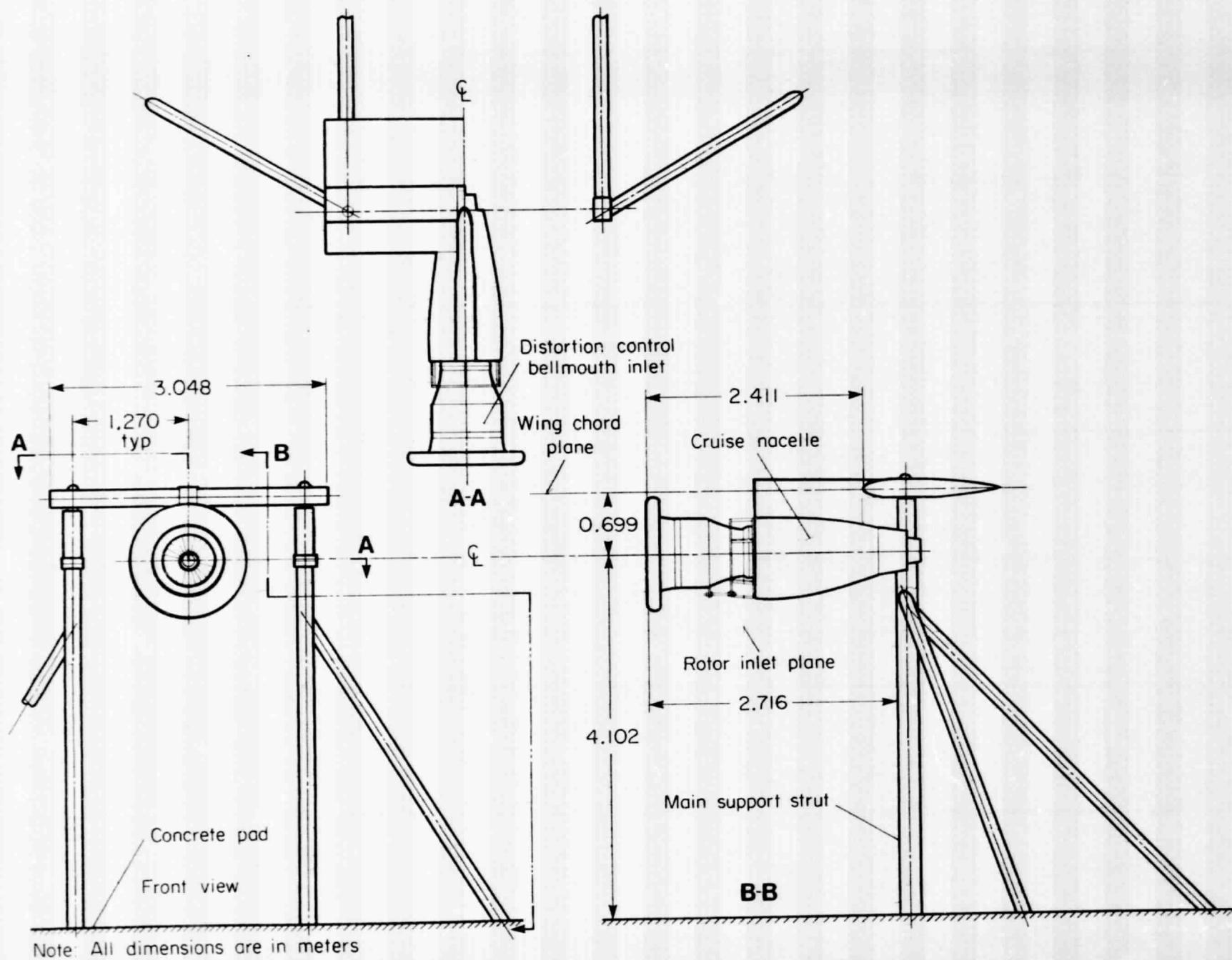


Figure 2.- General arrangement of JT15D-1 static test installation.

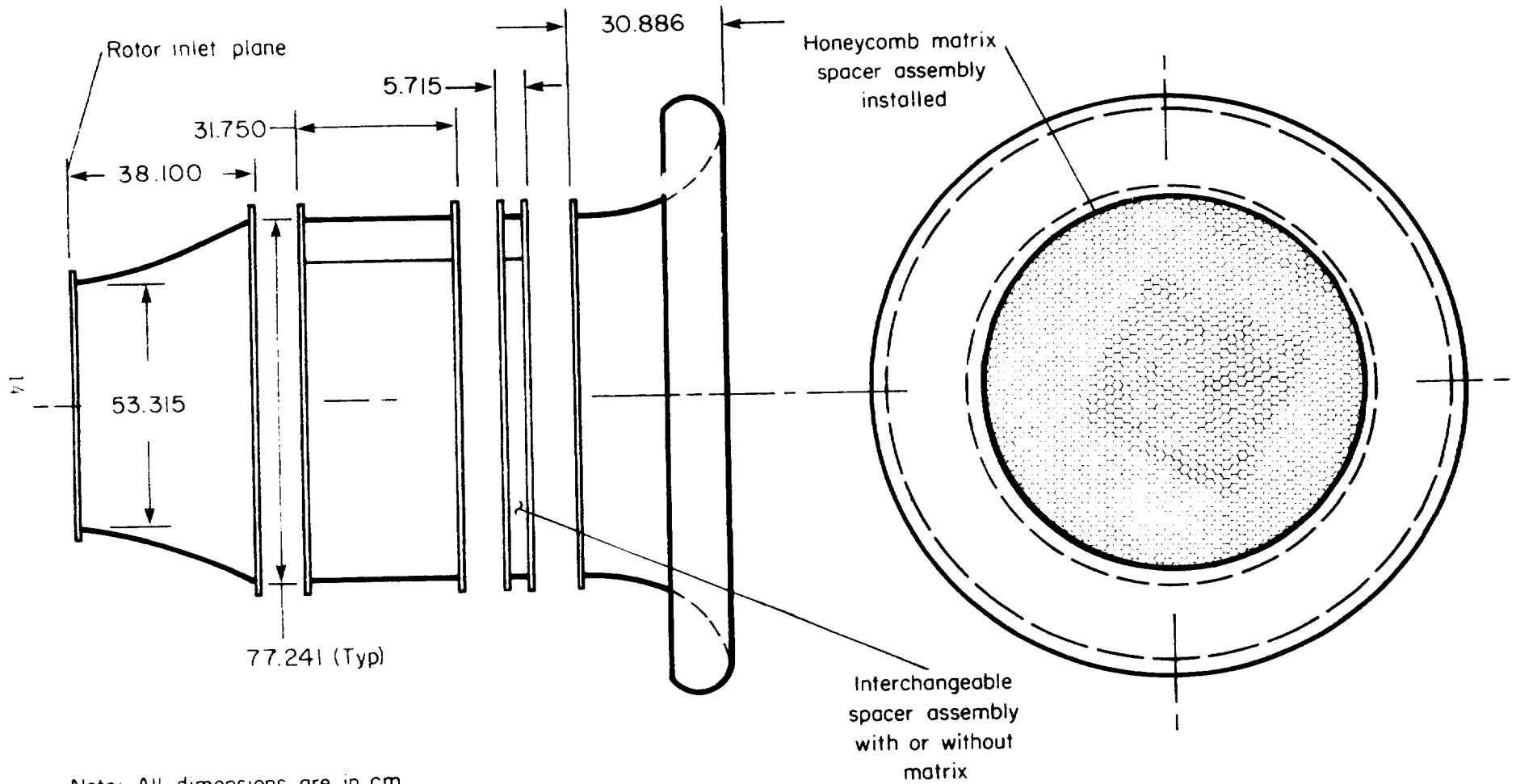


Figure 3.- Distortion control bellmouth inlet.

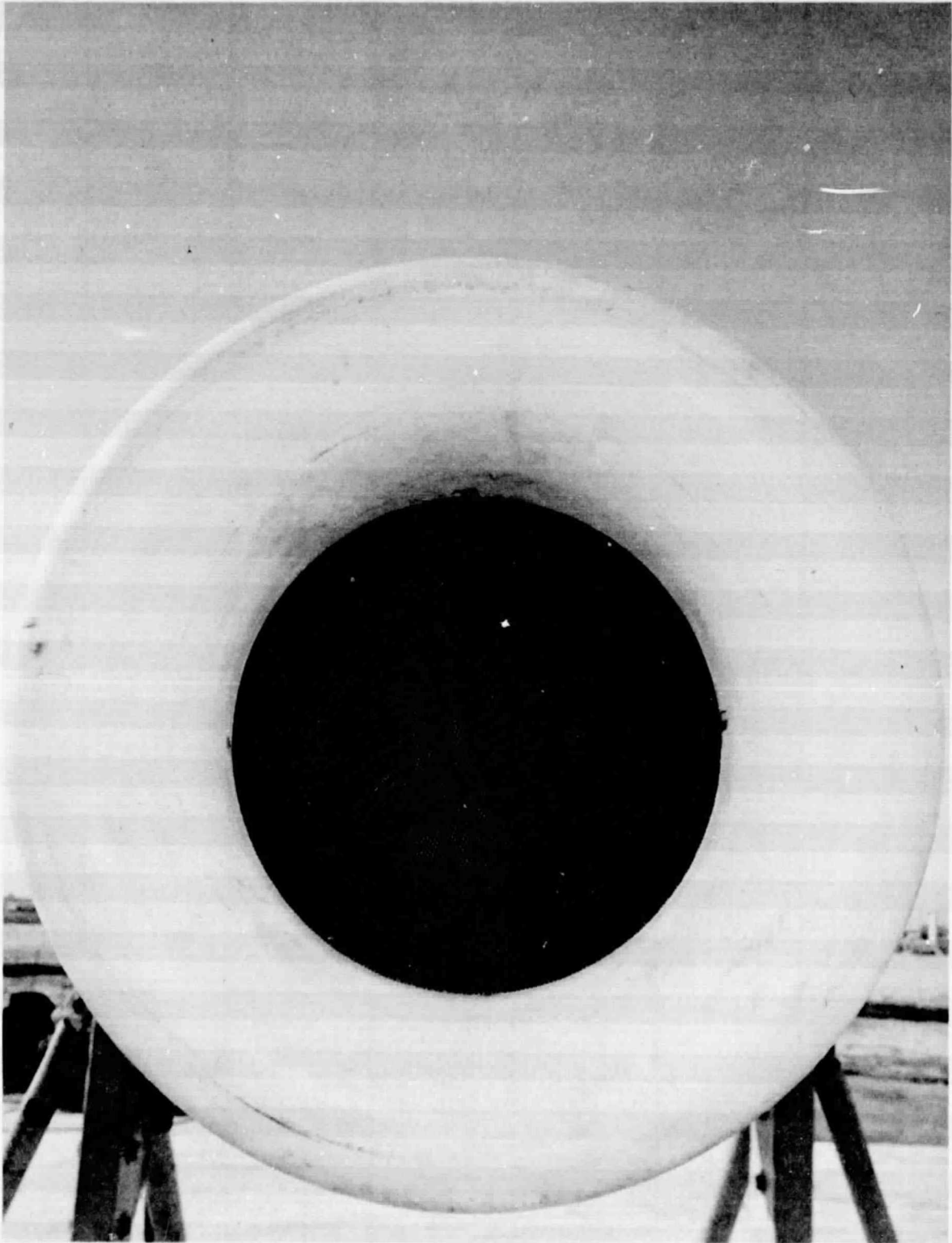


Figure 4.- Photograph of honeycomb matrix installation in distortion control bellmouth inlet.

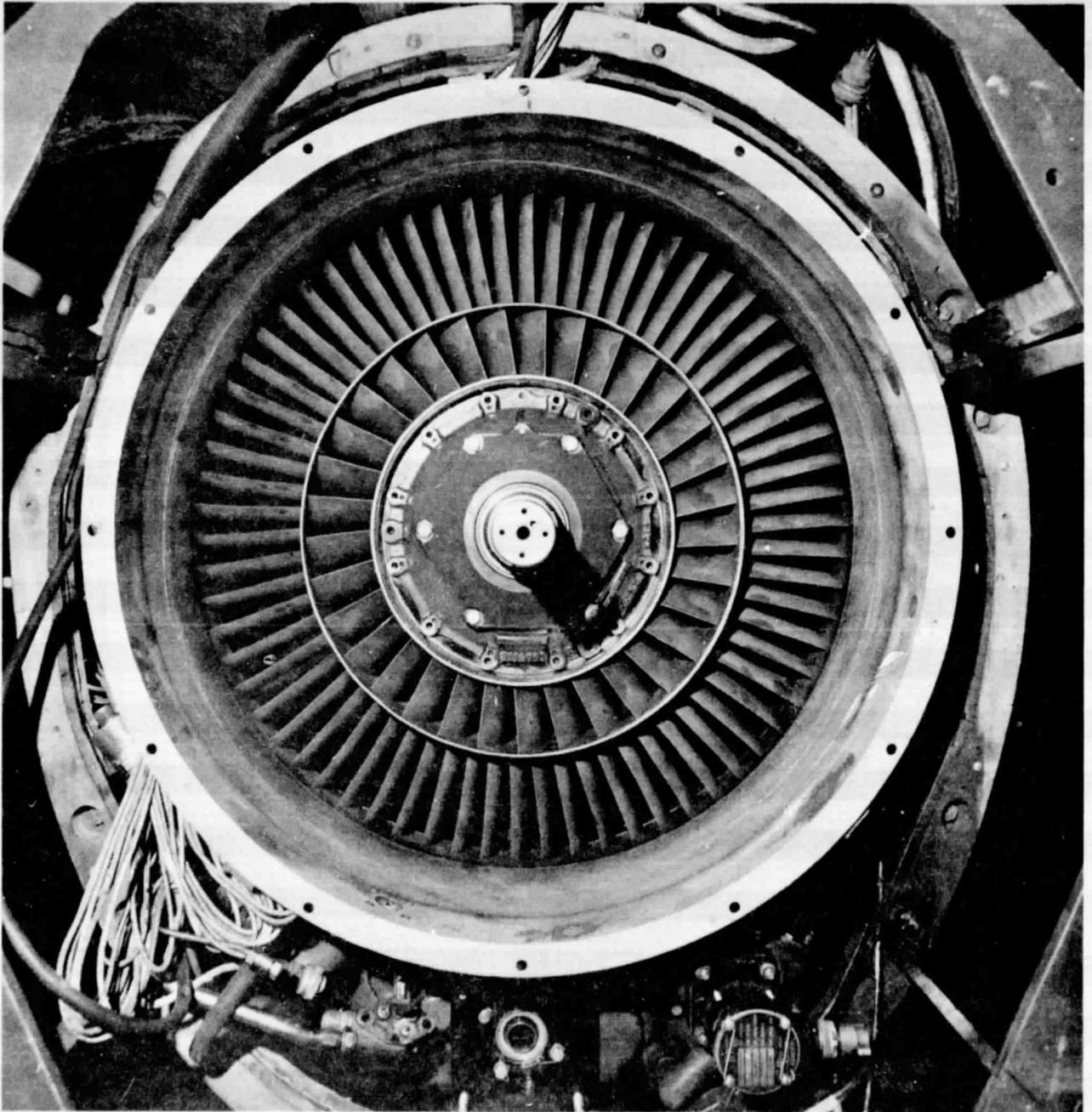


Figure 5.- Photograph of production JT15D-1 fan outlet guide vane stator assembly.

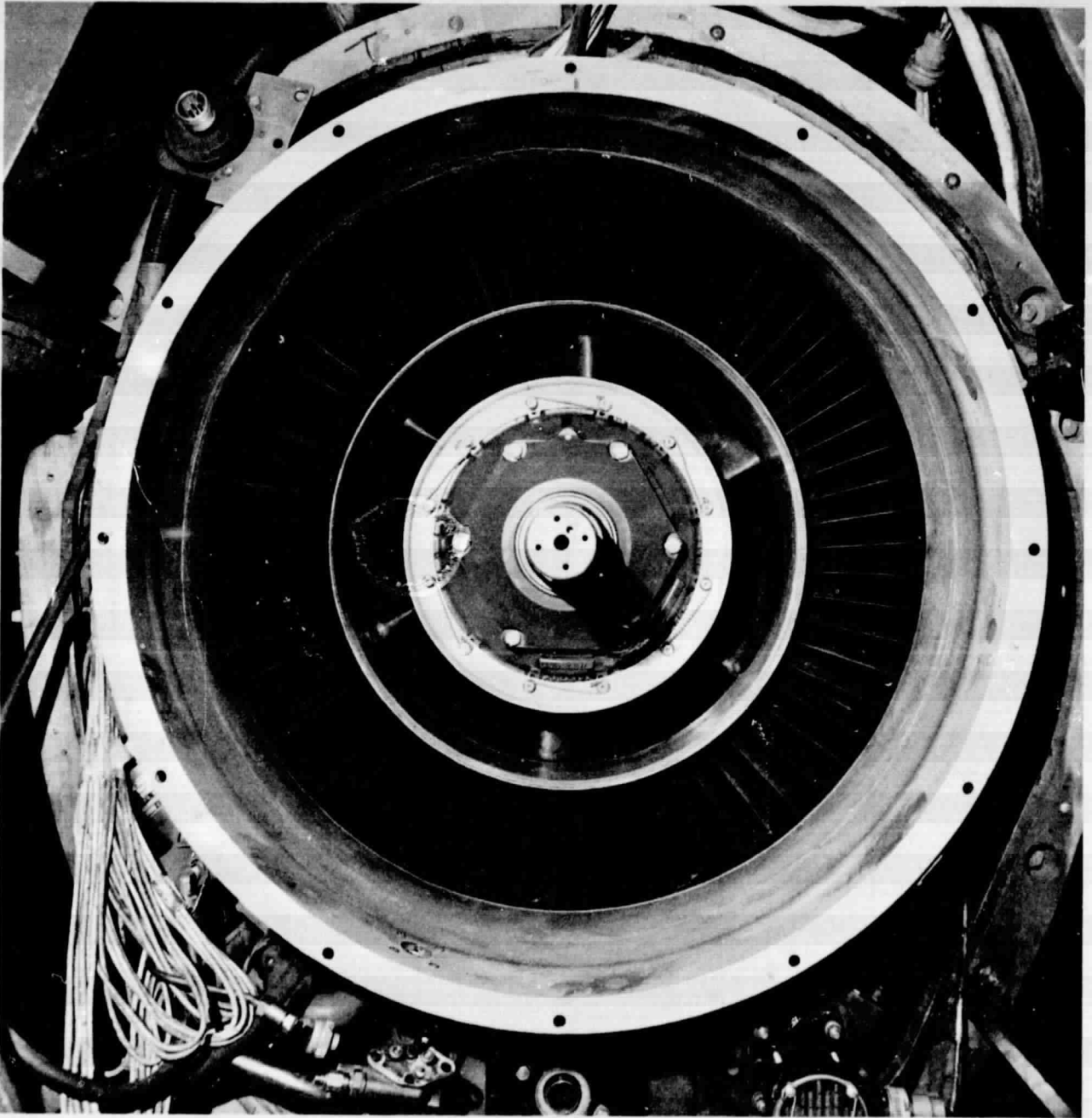


Figure 6.- Photograph of modified JT15D-1 fan outlet guide stator assembly.

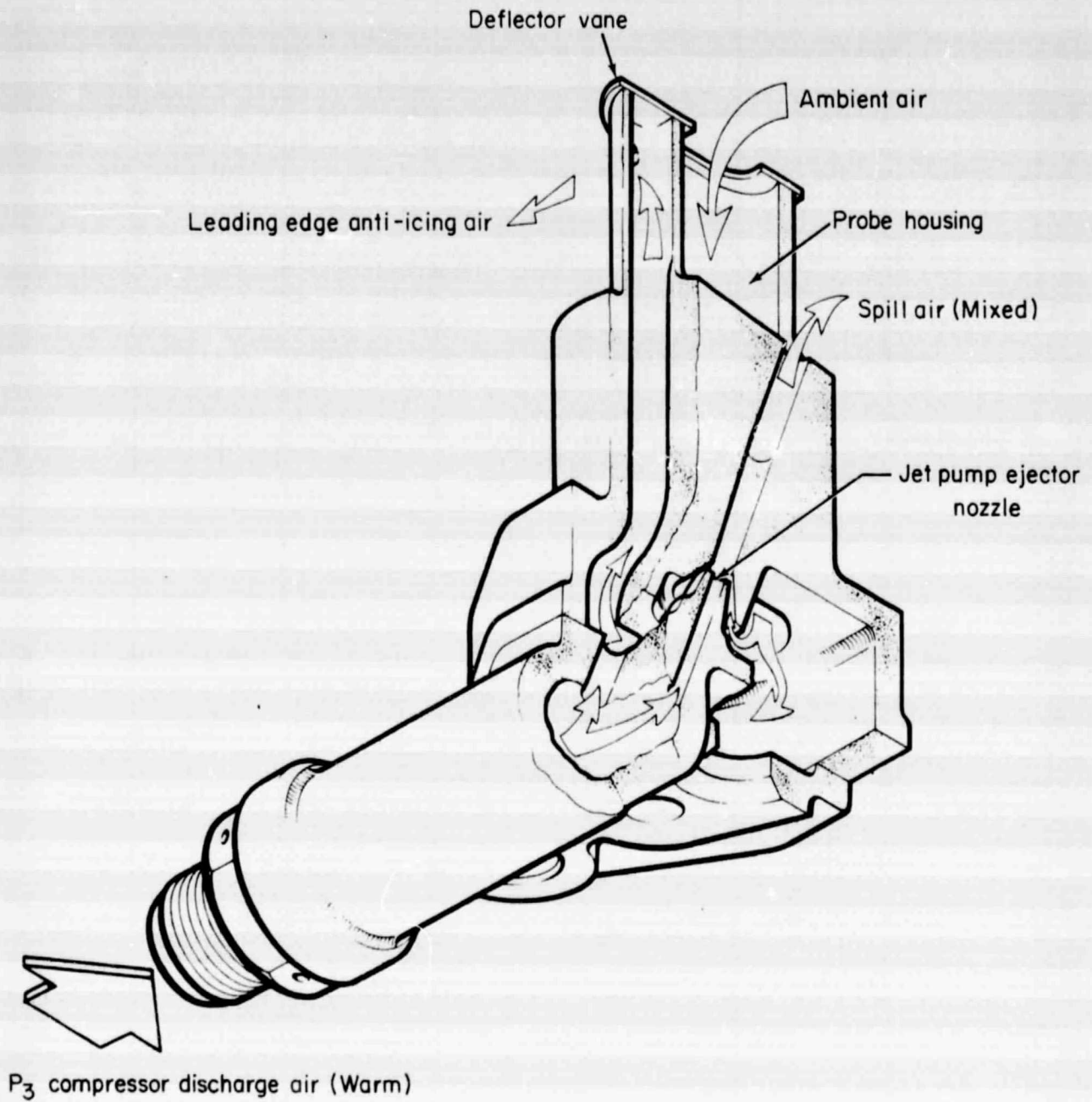


Figure 7.- Operating schematic of production JT15D-1 T<sub>1</sub> probe (from ref. 3).

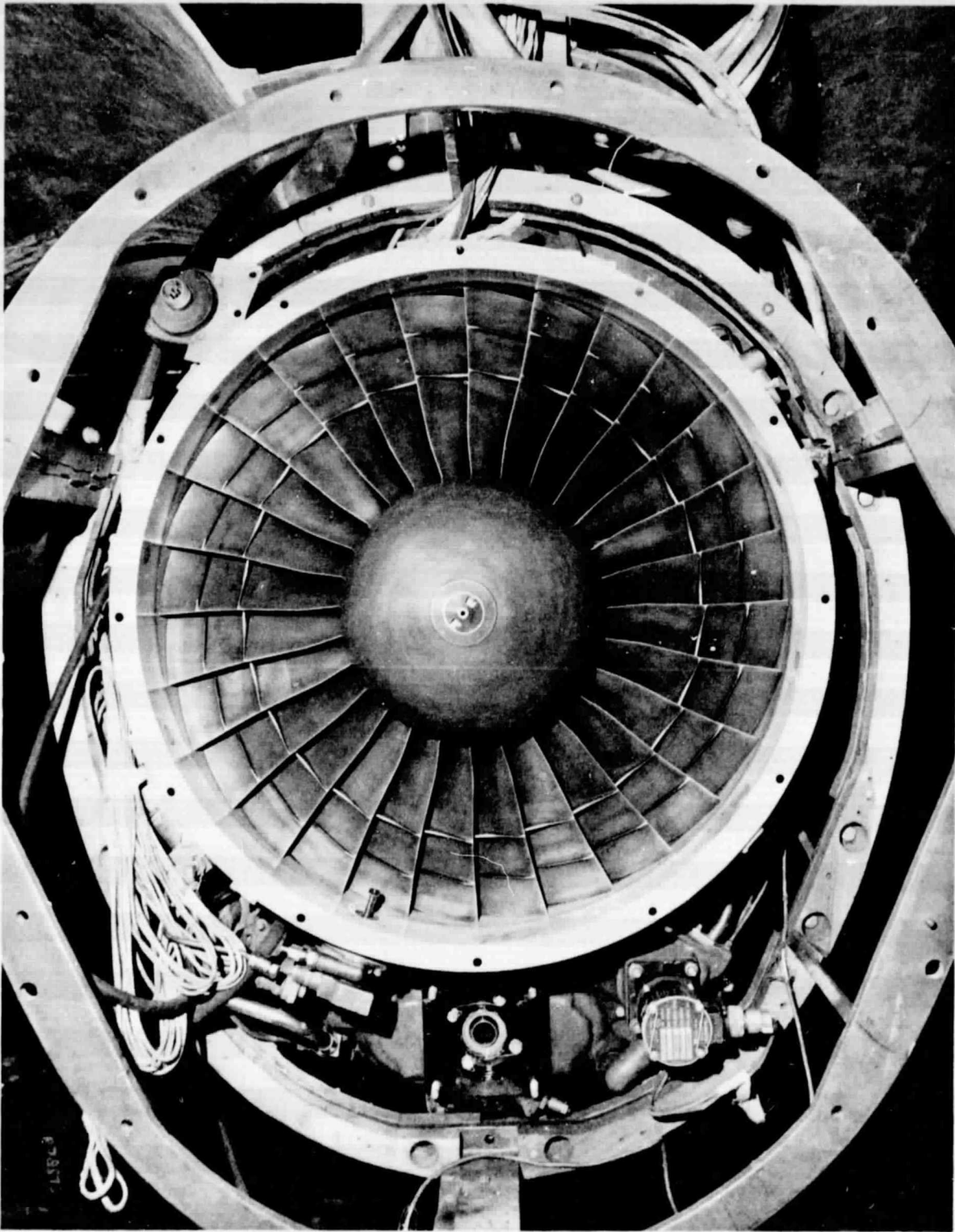


Figure 8.- Photograph of production JT15D-1 inlet temperature-sensing probe installation.

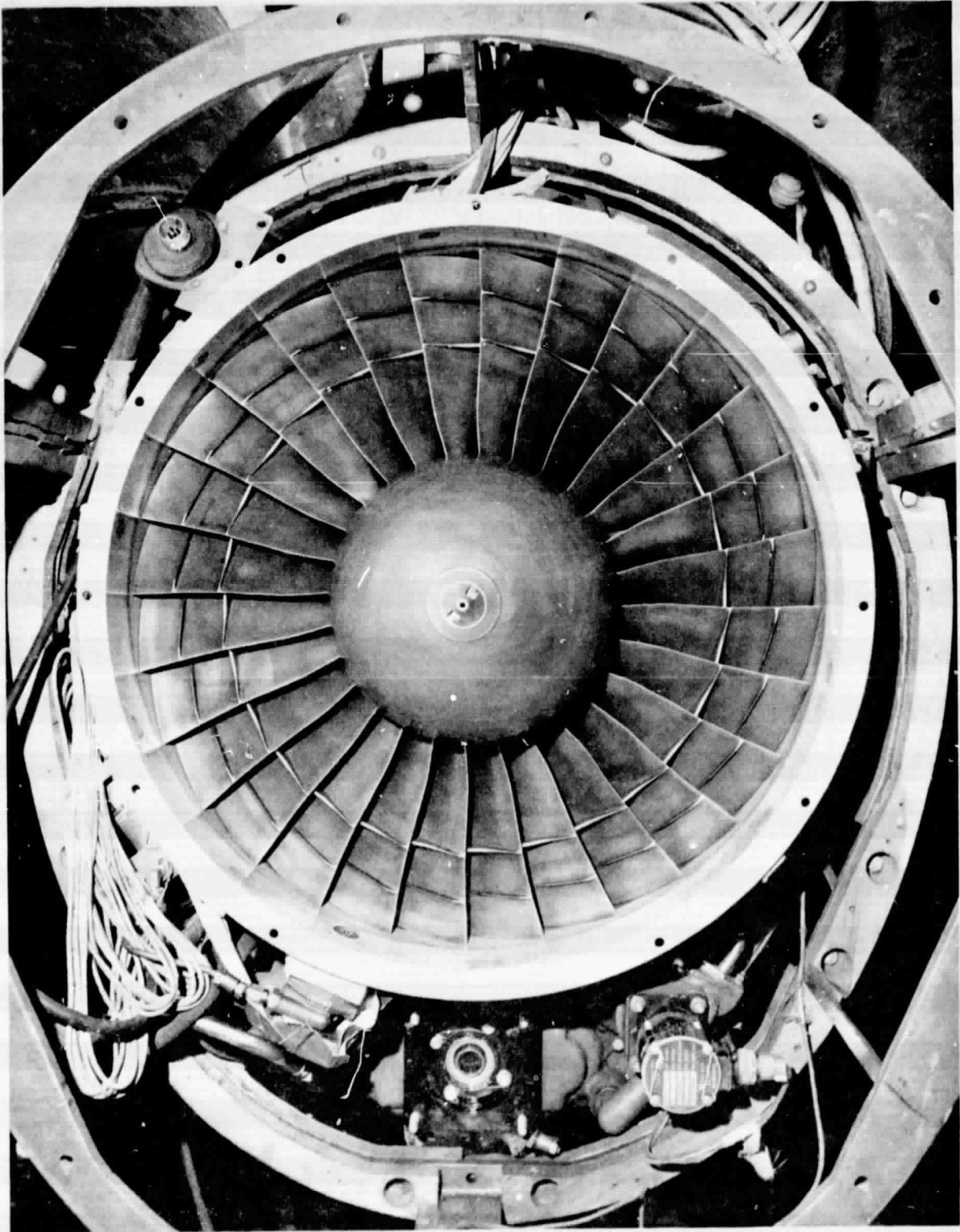


Figure 9.- Photograph of modified JT15D-1 inlet temperature-sensing probe installation.

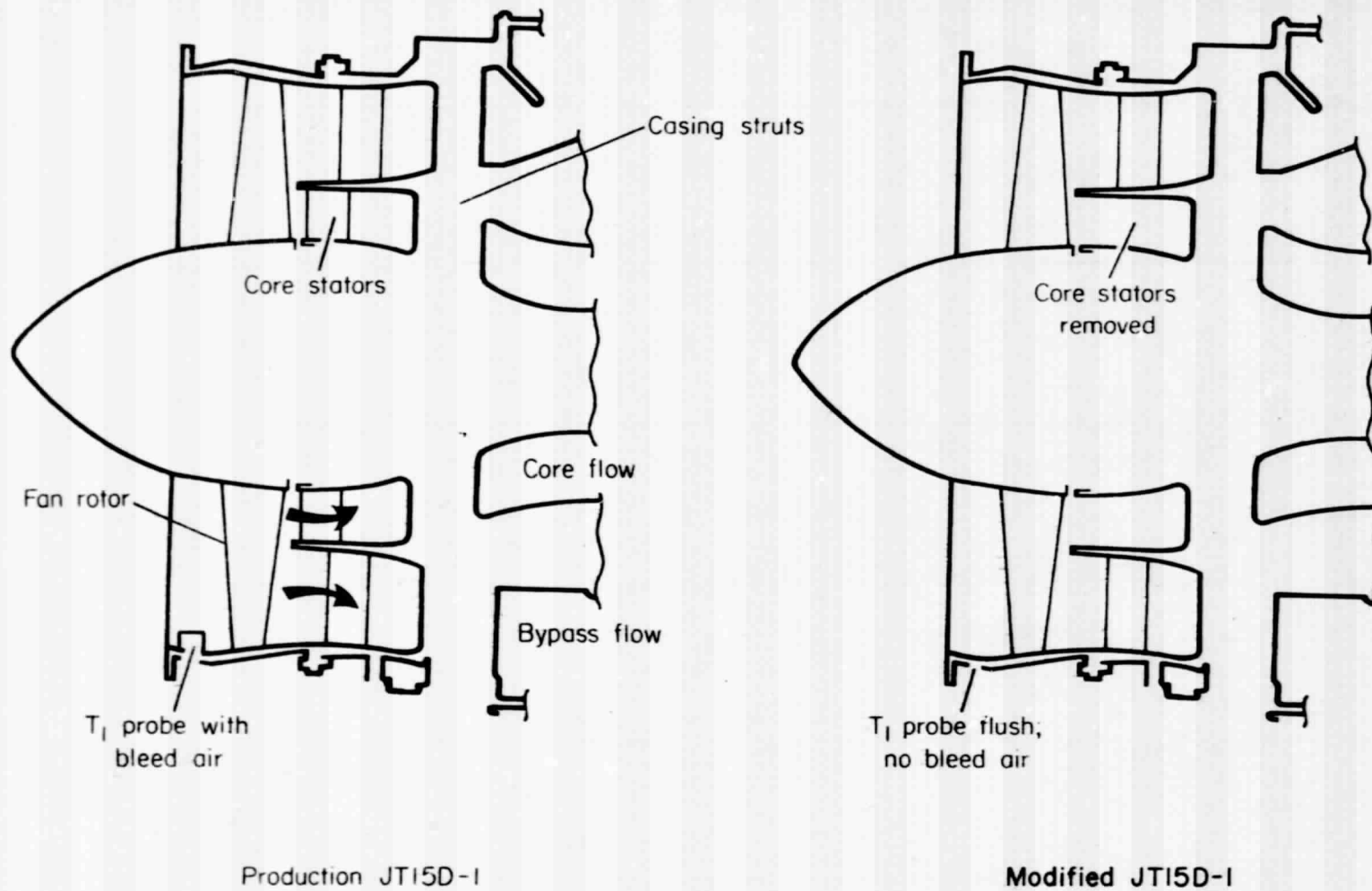


Figure 10.- Schematic of JT15D-1 core-stator and  $T_1$  probe modifications.



Figure 11.- Photograph of JT15D-1 engine in cruise configuration installed in Ames 40- by 80-Foot Wind Tunnel.

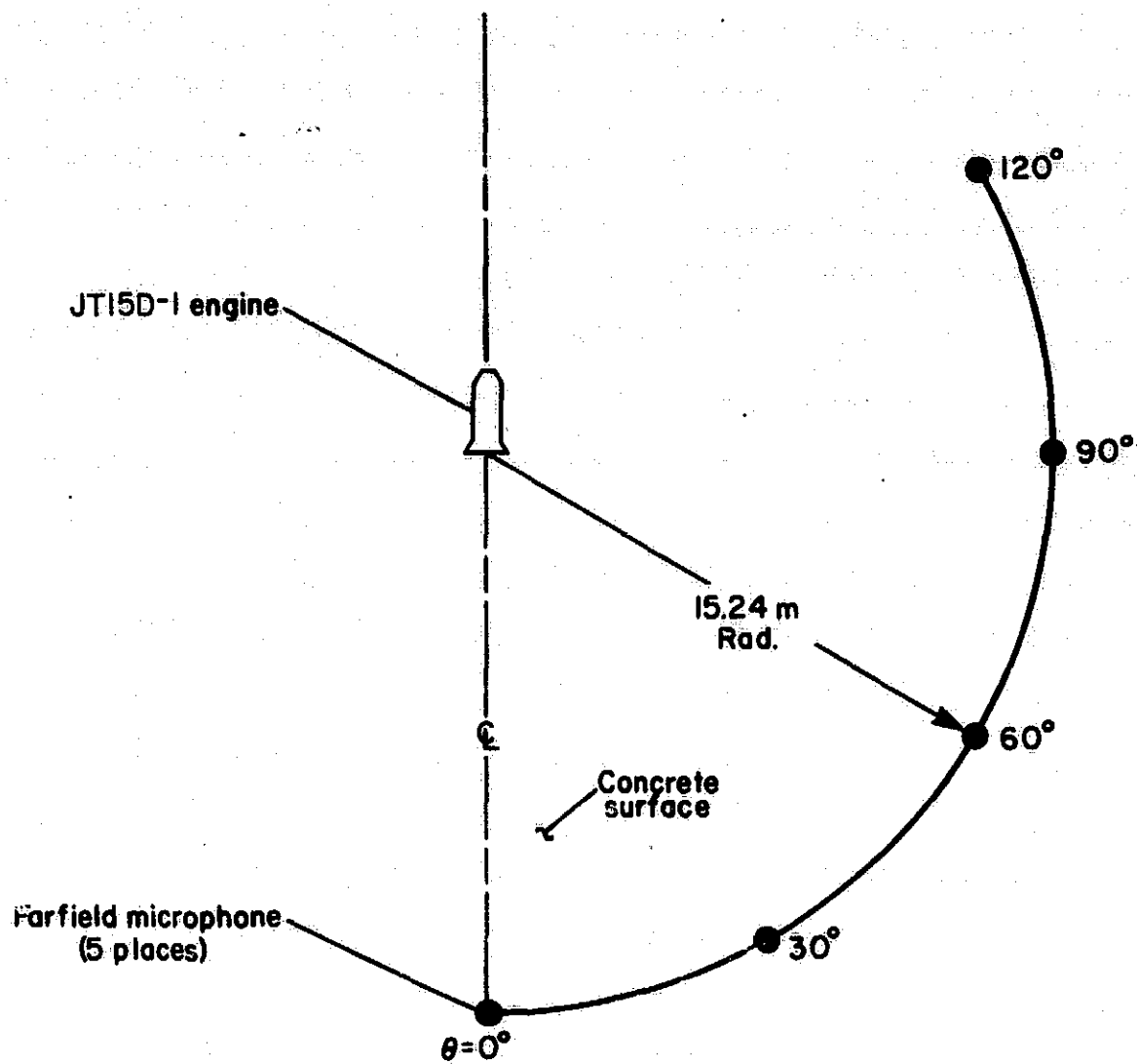
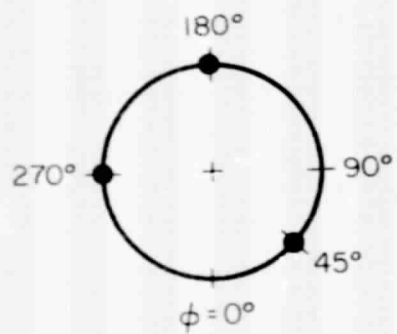
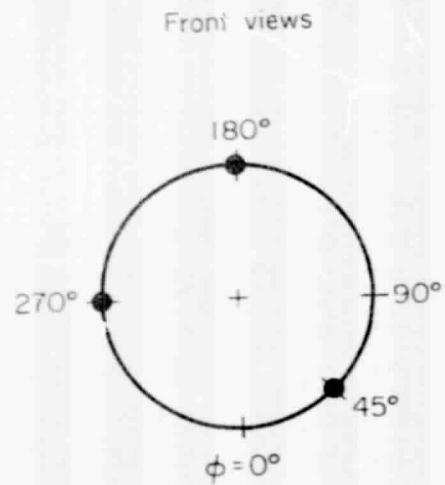


Figure 12.- Test engine and far-field microphone arrangement.



● Duct microphone

Note: All dimensions are in cm

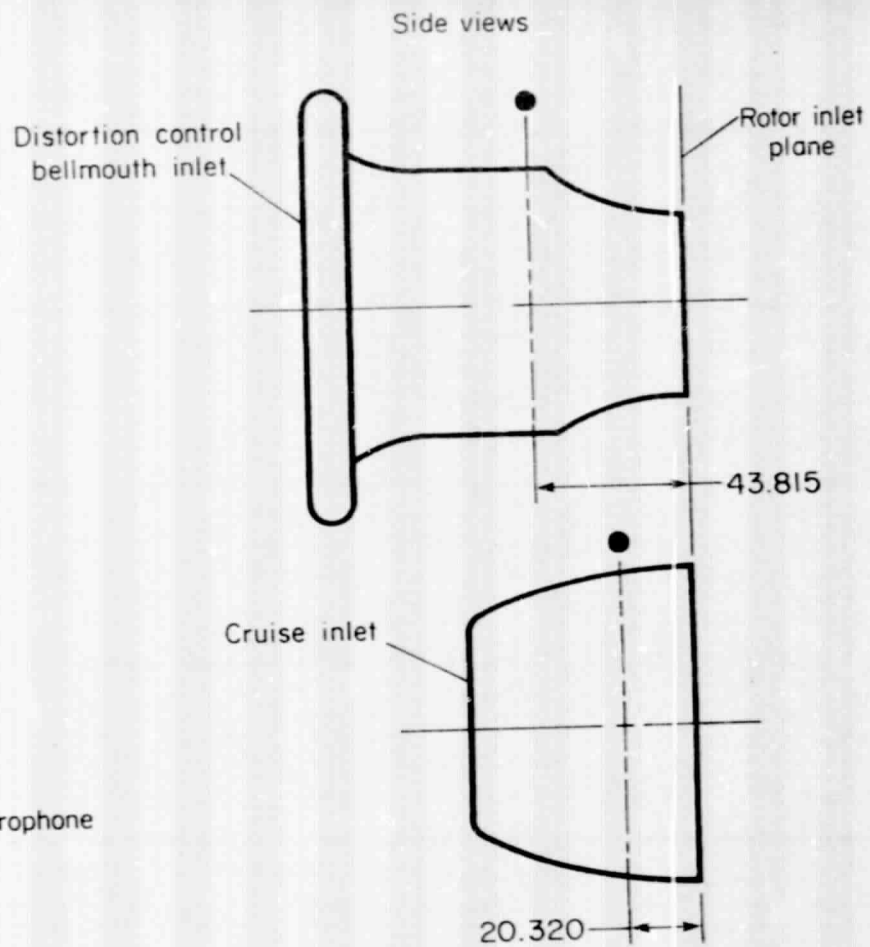
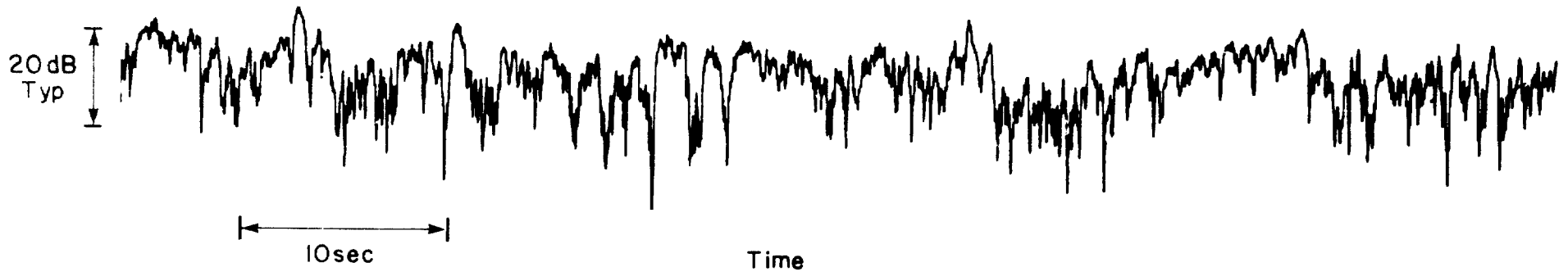
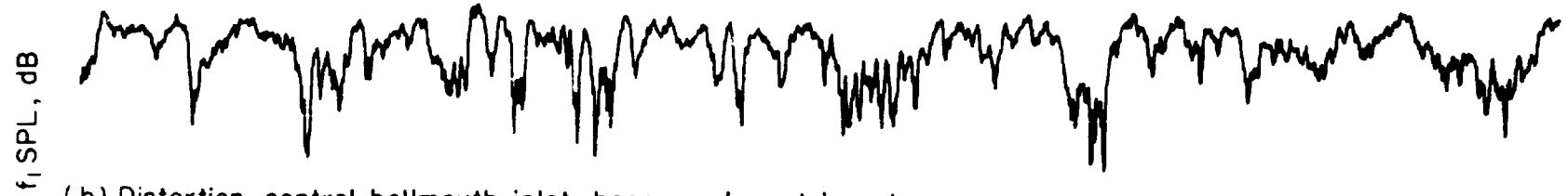


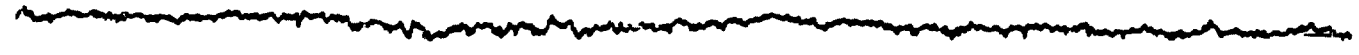
Figure 13.- Location of fan inlet-duct microphones.



(a) Standard bellmouth inlet



(b) Distortion control bellmouth inlet, honeycomb matrix out



(c) Distortion control bellmouth inlet, honeycomb matrix in ( $Z/d=8$ )



(d) Distortion control bellmouth inlet, honeycomb matrix in ( $Z/d=10$ )

Figure 14.- Effect of distortion-control bellmouth inlet on in-duct  $t_1$   
 SPL variability from reference 1, figure 13:  $\phi = 180^\circ$ ;  
 fan rpm<sub>n</sub> = 10,230; h/D = 6.5.

REPRODUCIBILITY OF THE ORIGINAL PAGE IS POOR

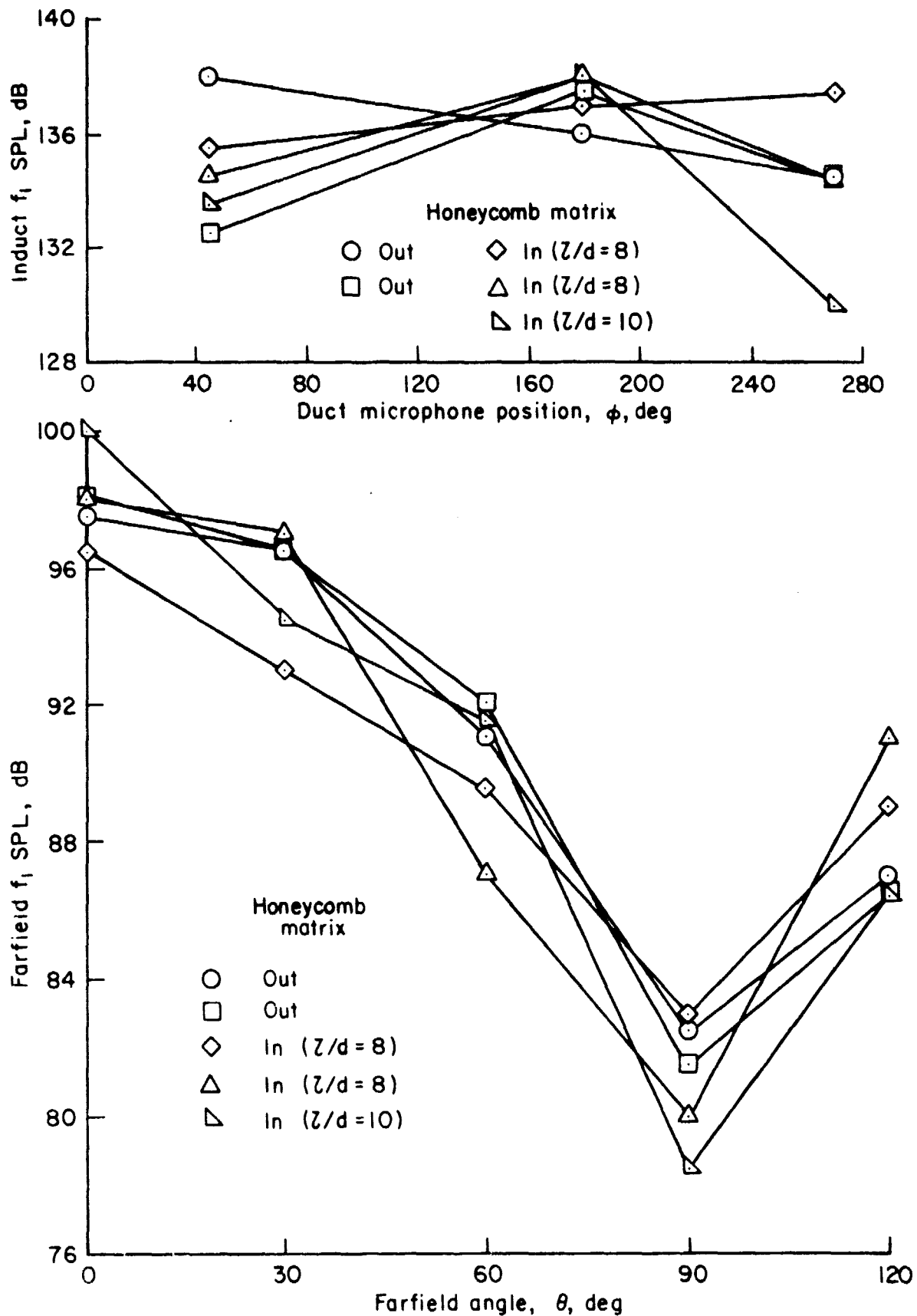


Figure 15.- Effect of distortion-control bellmouth inlet on  $f_1$  SPL from reference 1, figure 14: fan rpm<sub>n</sub> = 10,230; h/D = 6.5; 40<sup>1</sup>sec sample.

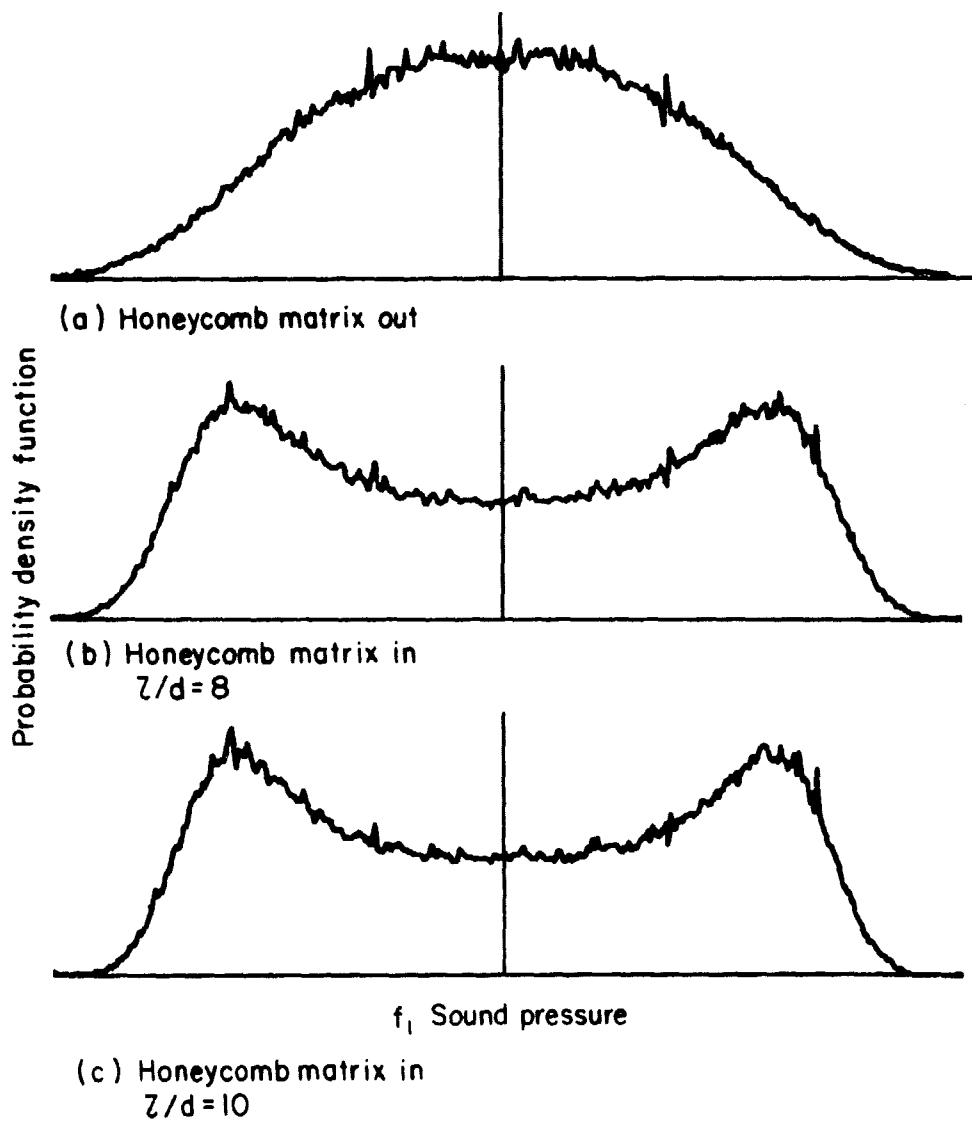


Figure 16.- Effect of distortion-control bellmouth inlet on probability density of  $f_1$  SPL from reference 1, figure 16: fan rpm<sub>n</sub> = 10,230;  $\phi = 180^\circ$ ;  $h/D = 6.5$ .

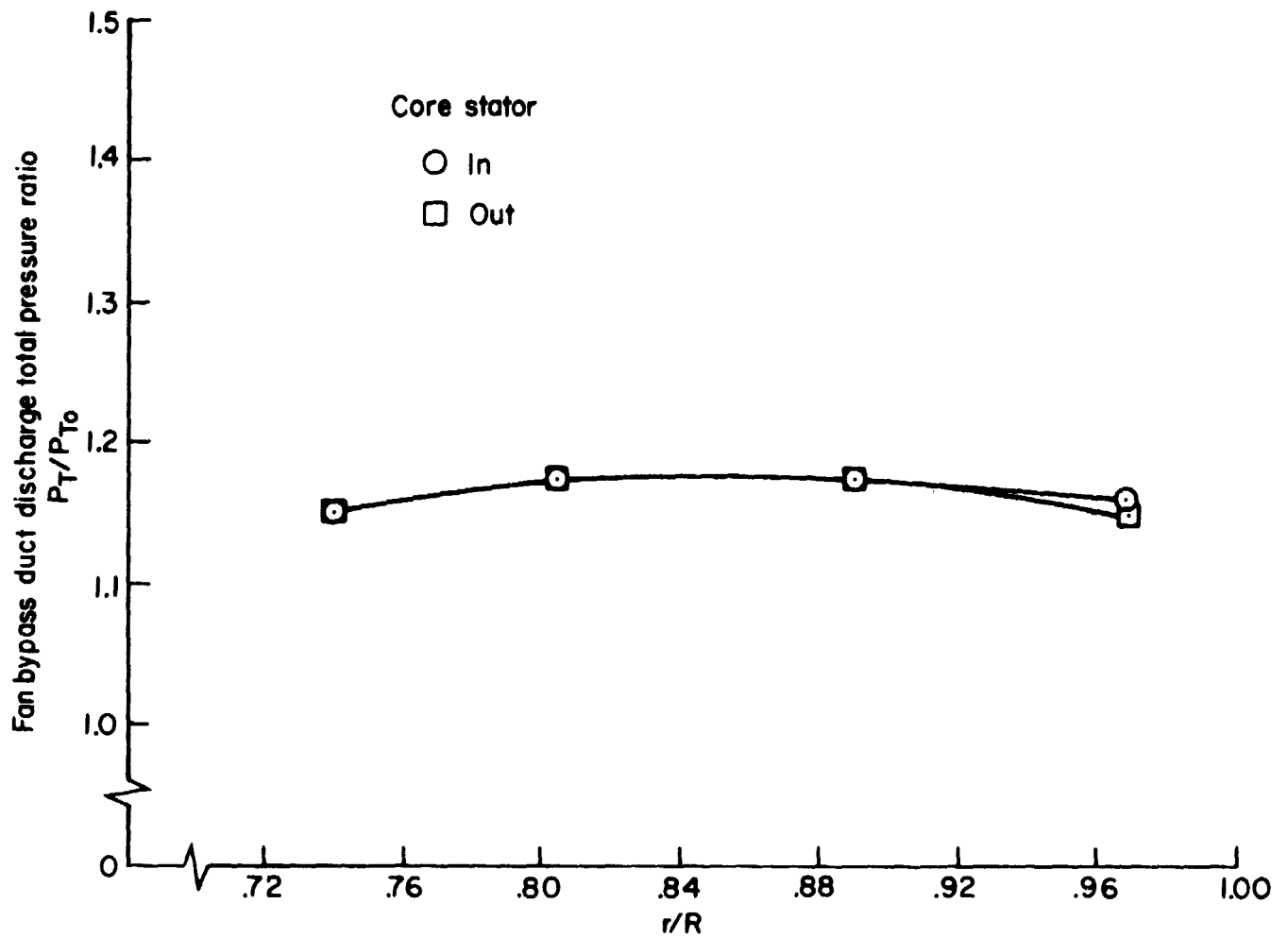


Figure 17.- Effect of removing the fan core stator on fan bypass flow total pressure rise:  
fan rpm<sub>n</sub> = 10,230; honeycomb out.

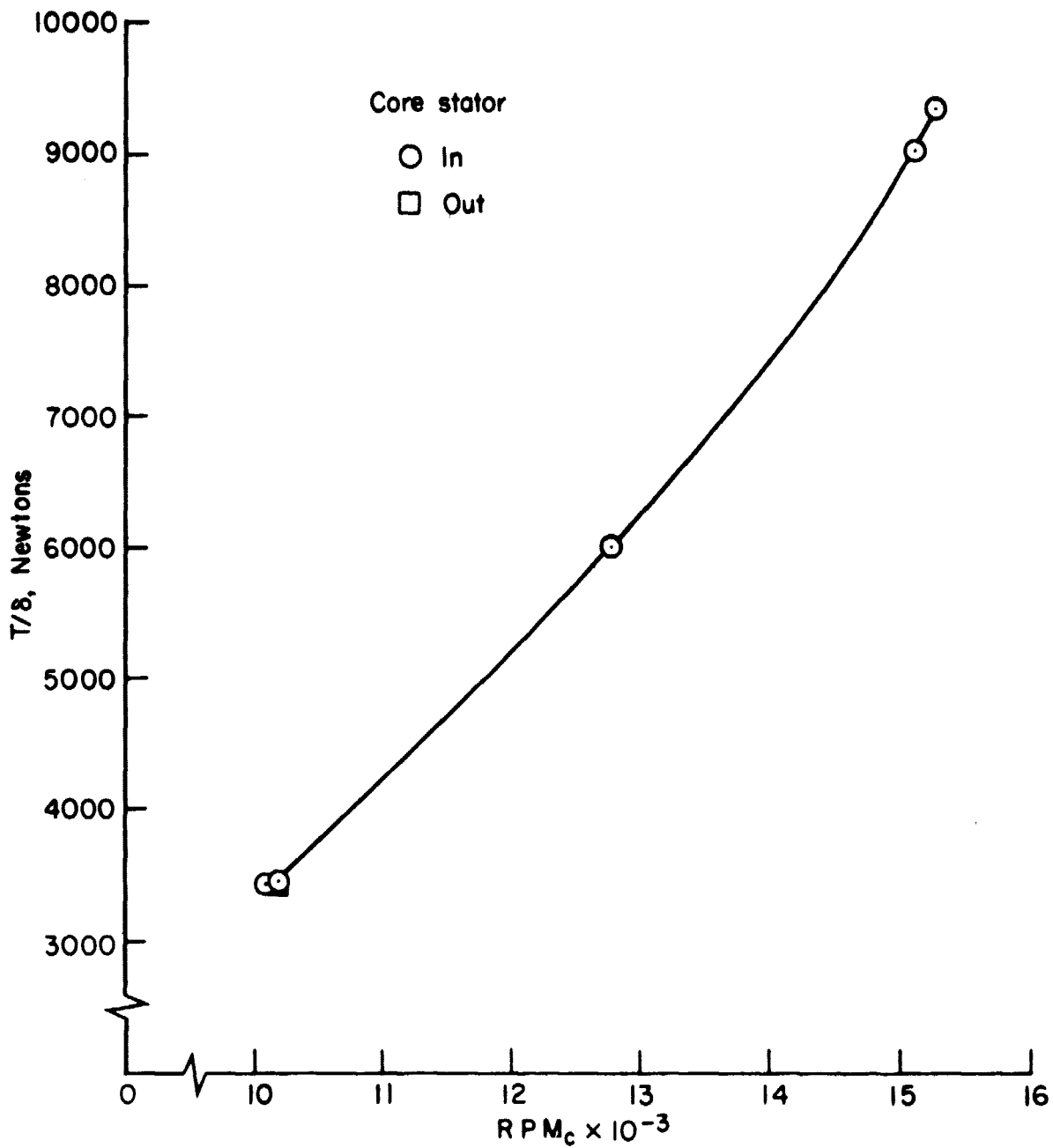
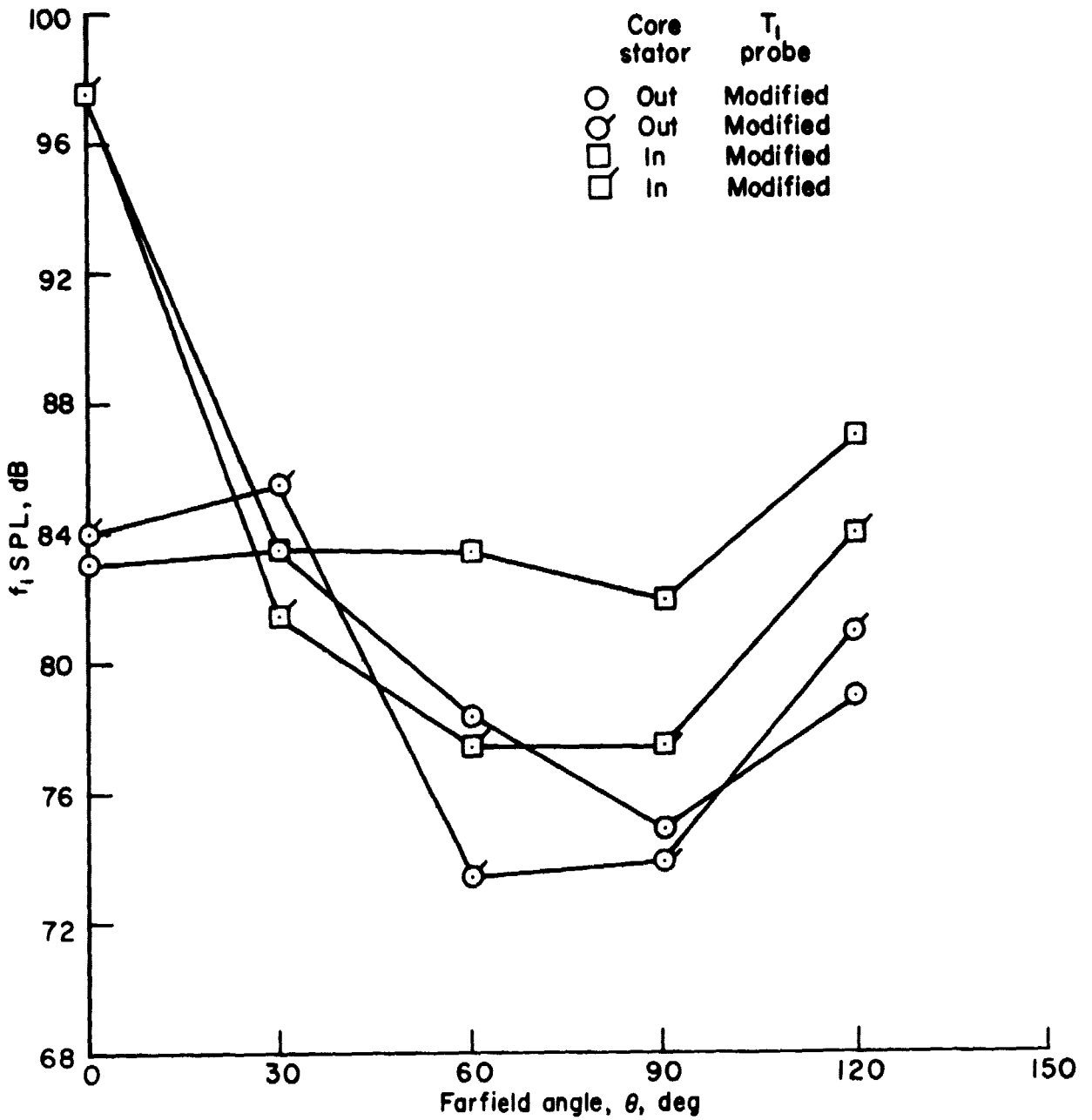
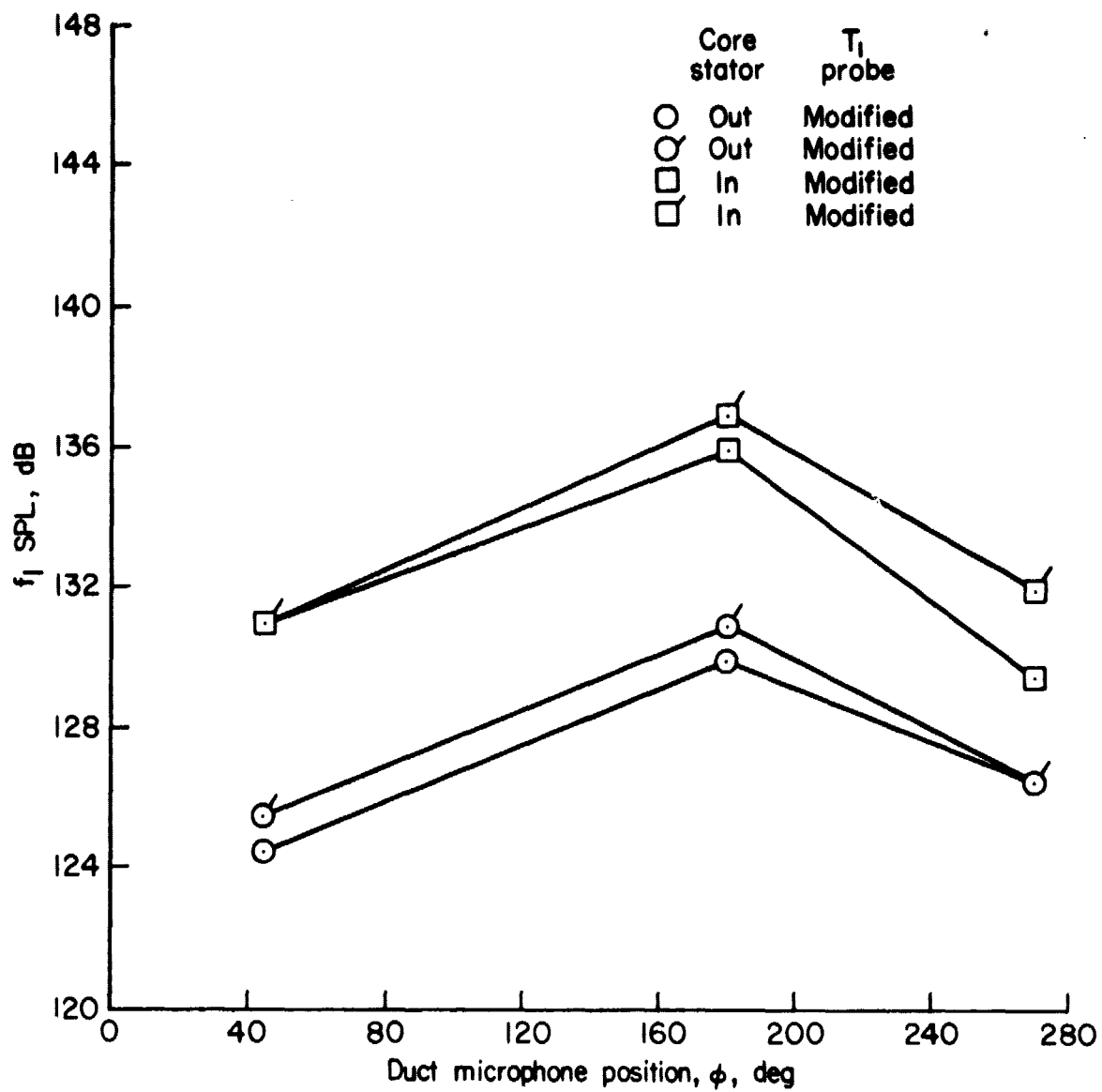


Figure 18.- Effect of removing the fan core stator on engine thrust.



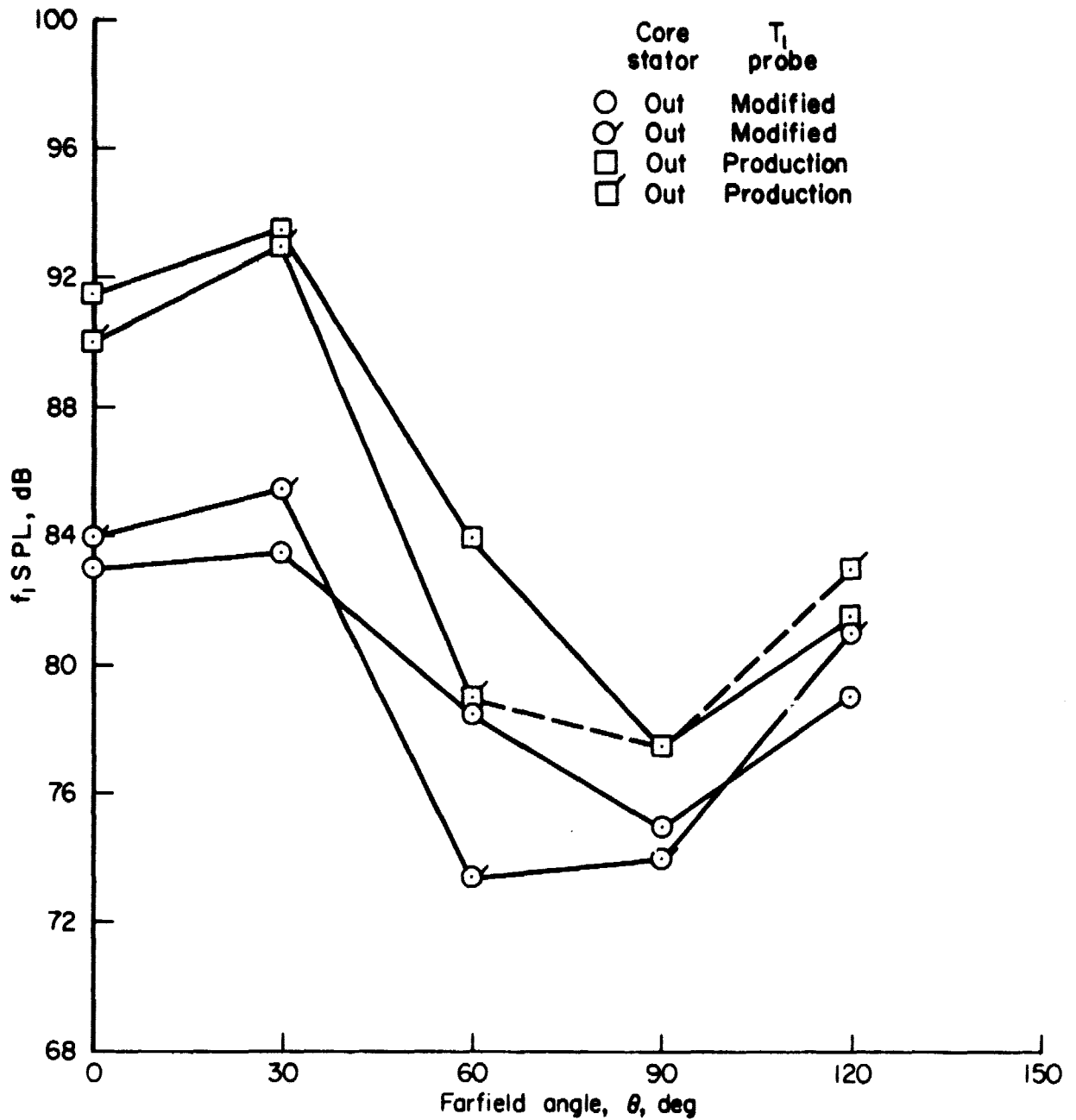
(a) Far-field  $f_1$  SPL.

Figure 19.- Effect of core stator on  $f_1$  SPL at approach power: fan  $rpm_n = 10,230$ ; distortion control inlet (honeycomb in); 40-sec sample.



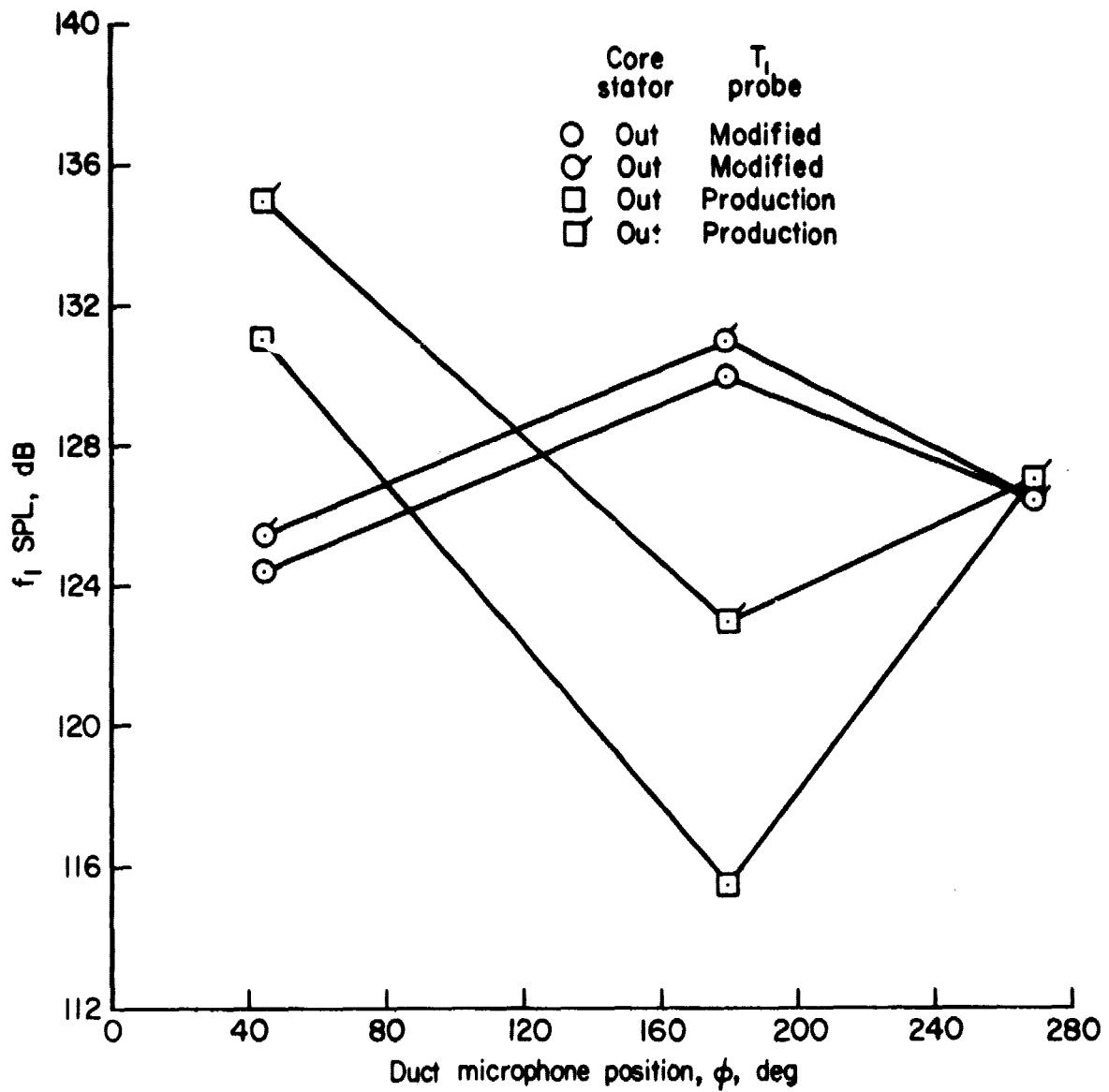
(b) In-duct  $f_1$  SPL.

Figure 19.- Concluded.



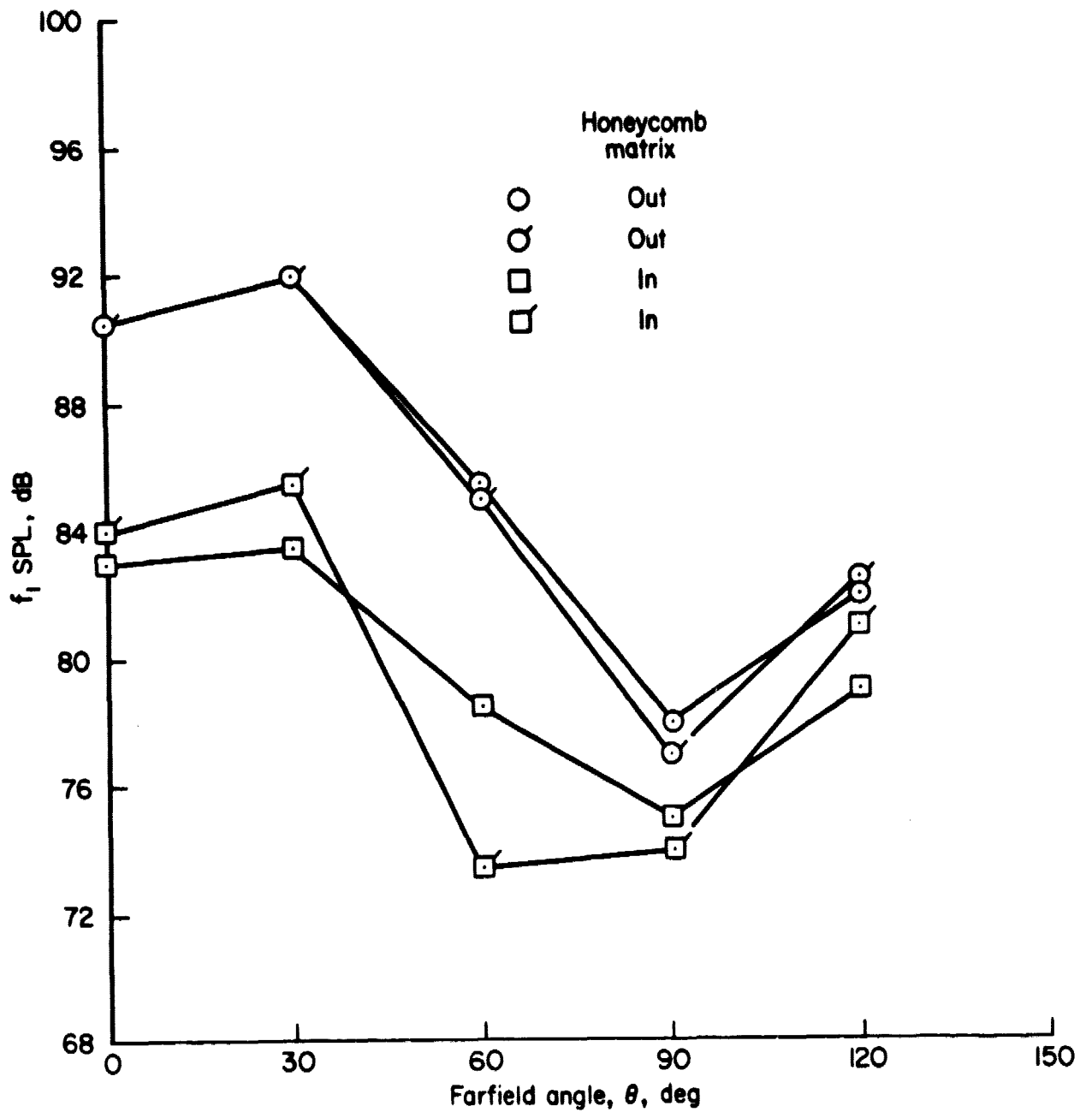
(a) Farfield  $f_1$  SPL

Figure 20.- Effect of  $T_1$  probe on  $f_1$  SPL at approach power: fan  $\text{rpm}_n = 10,230$ ; distortion control inlet (honeycomb in); 40-sec sample.



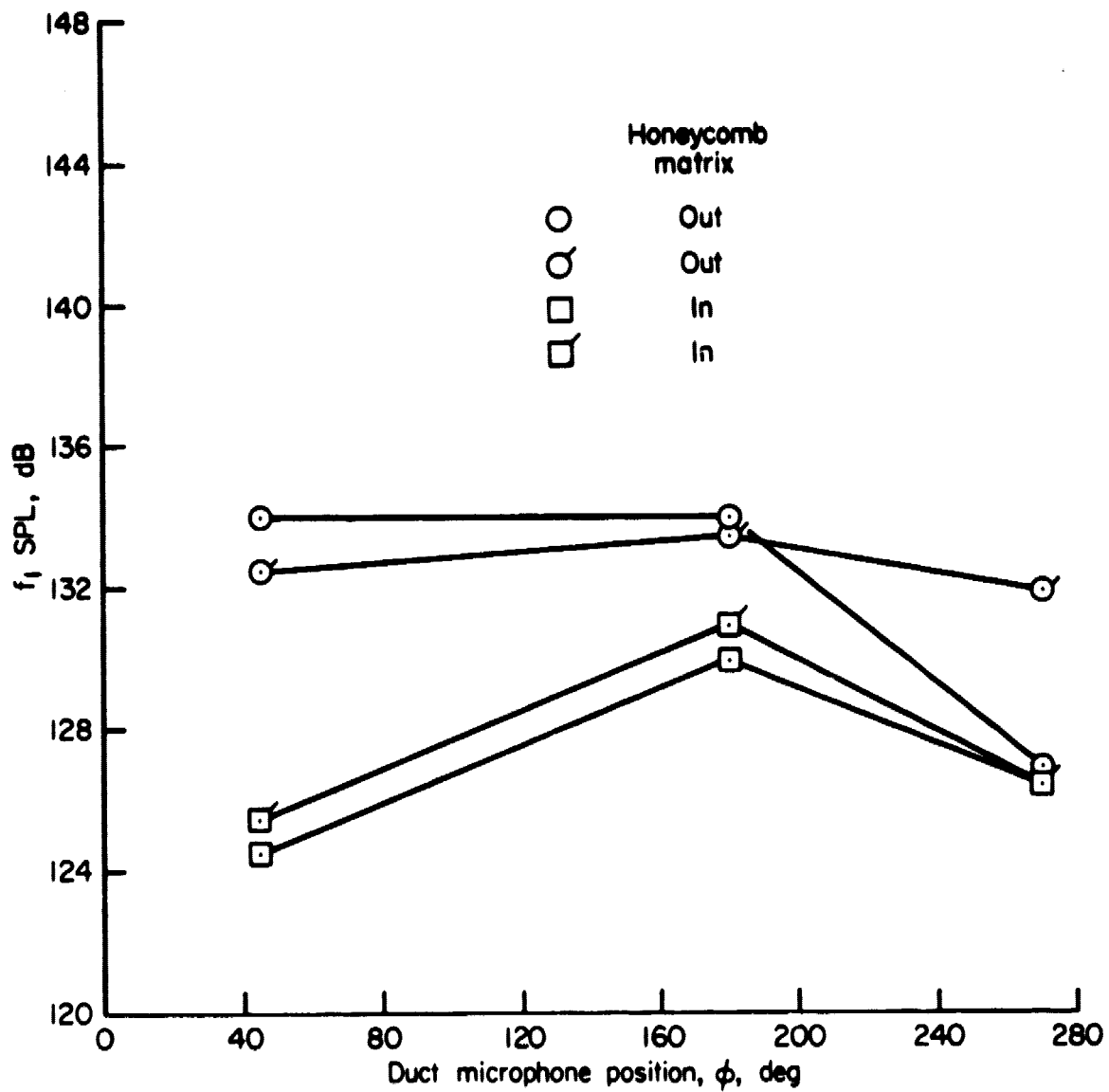
(b) In-duct  $f_1$  SPL.

Figure 20.- Concluded.



(a) Farfield  $f_1$  SPL

Figure 21.- Effect of atmospheric turbulence on  $f_1$  SPL at approach power: fan rpm<sub>n</sub> = 10,230; distortion control inlet; core stator out; modified  $T_1$  probe; 40-sec sample.



(b) In-duct  $f_1$  SPL.

Figure 21.- Concluded.

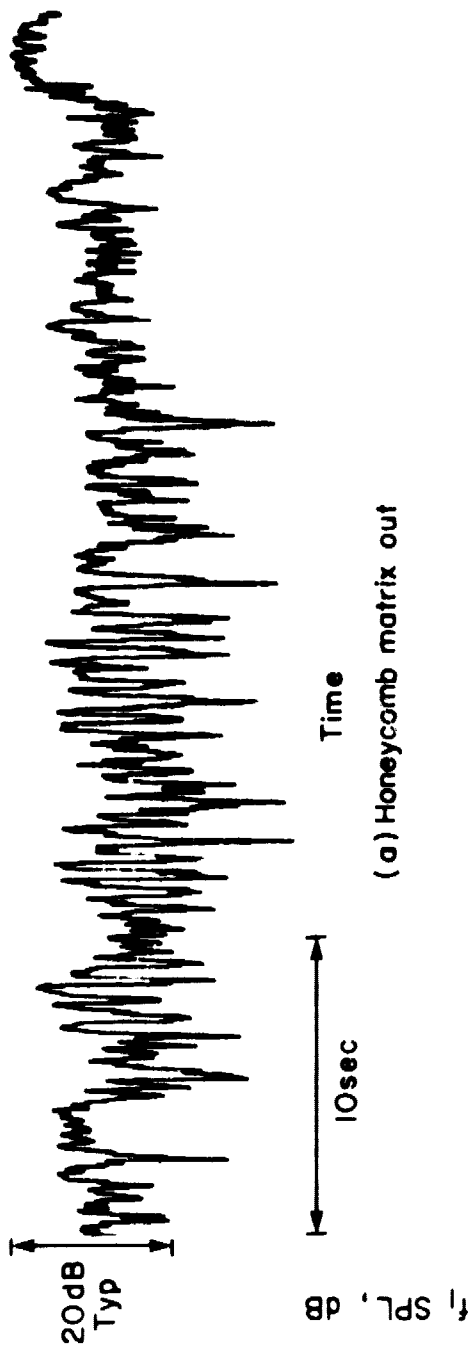


Figure 22.- Effect of distortion-control bellmouth inlet on in-duct  $f_1$  SPL variability: core stator removed; modified  $T_1$  probe;  $\phi = 270^\circ$ ; fan rpm<sub>n</sub> = 10,230.

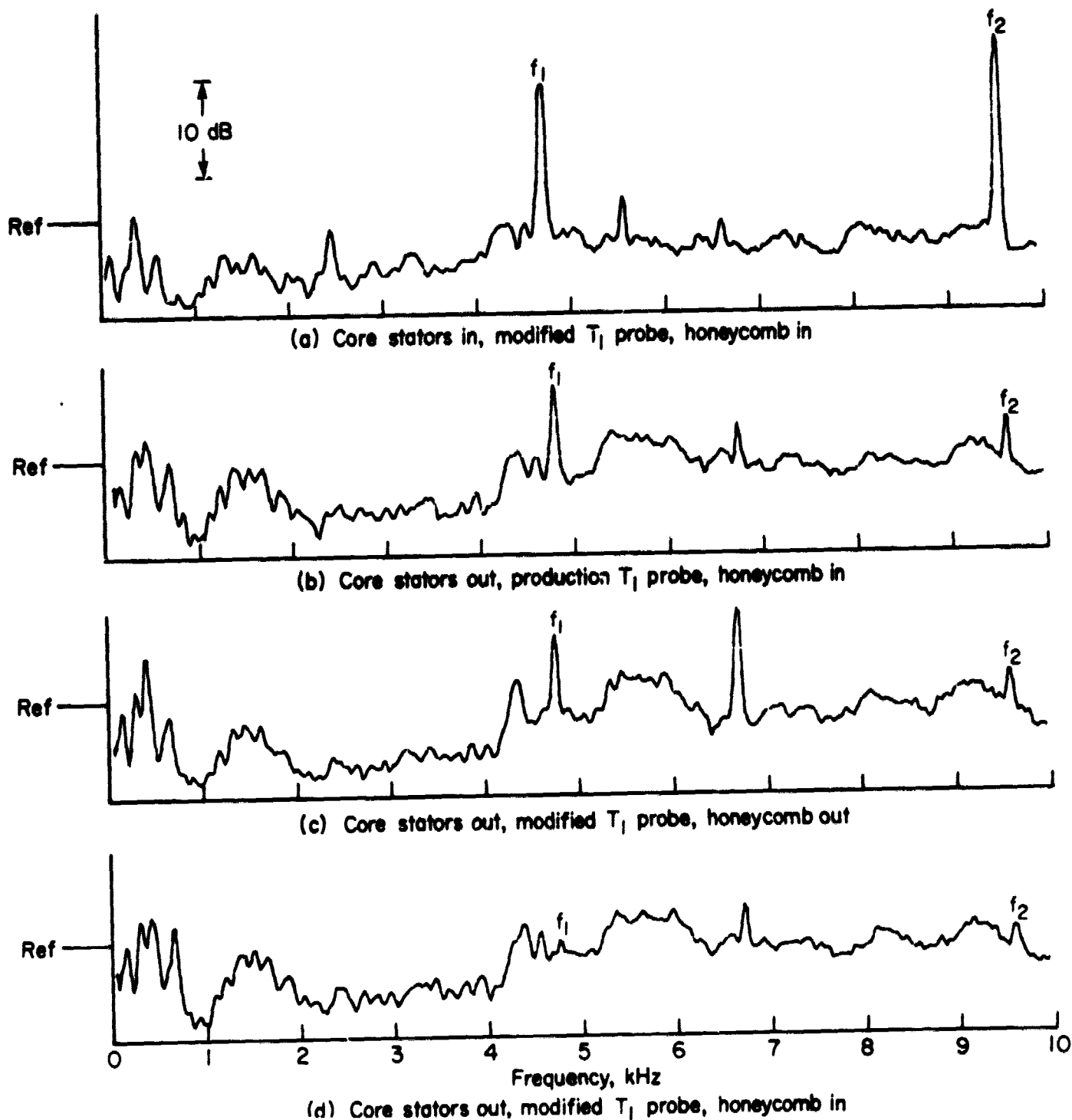


Figure 23.- Spectral analysis of on-axis contribution of core stators,  $T_1$  probe and atmospheric turbulence to  $f_1$  SPL:  $\text{rpm}_n = 10,230$ ; distortion control inlet; 40 sec sample.

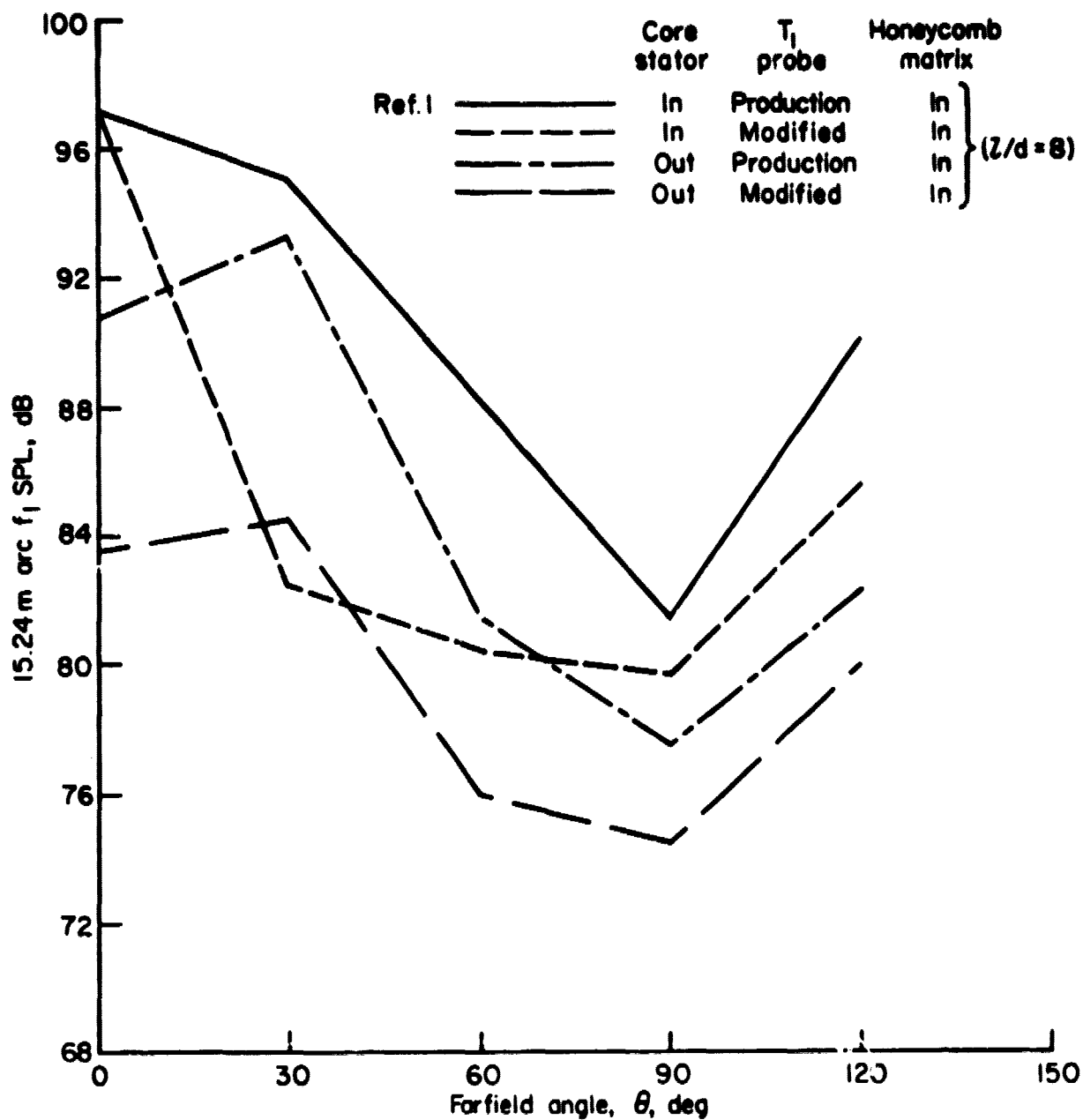


Figure 24.- Comparison of individual contributions to  $f_1$  SPL with total levels measured in reference 1: fan rpm<sub>n</sub> = 10,230; distortion control inlet.

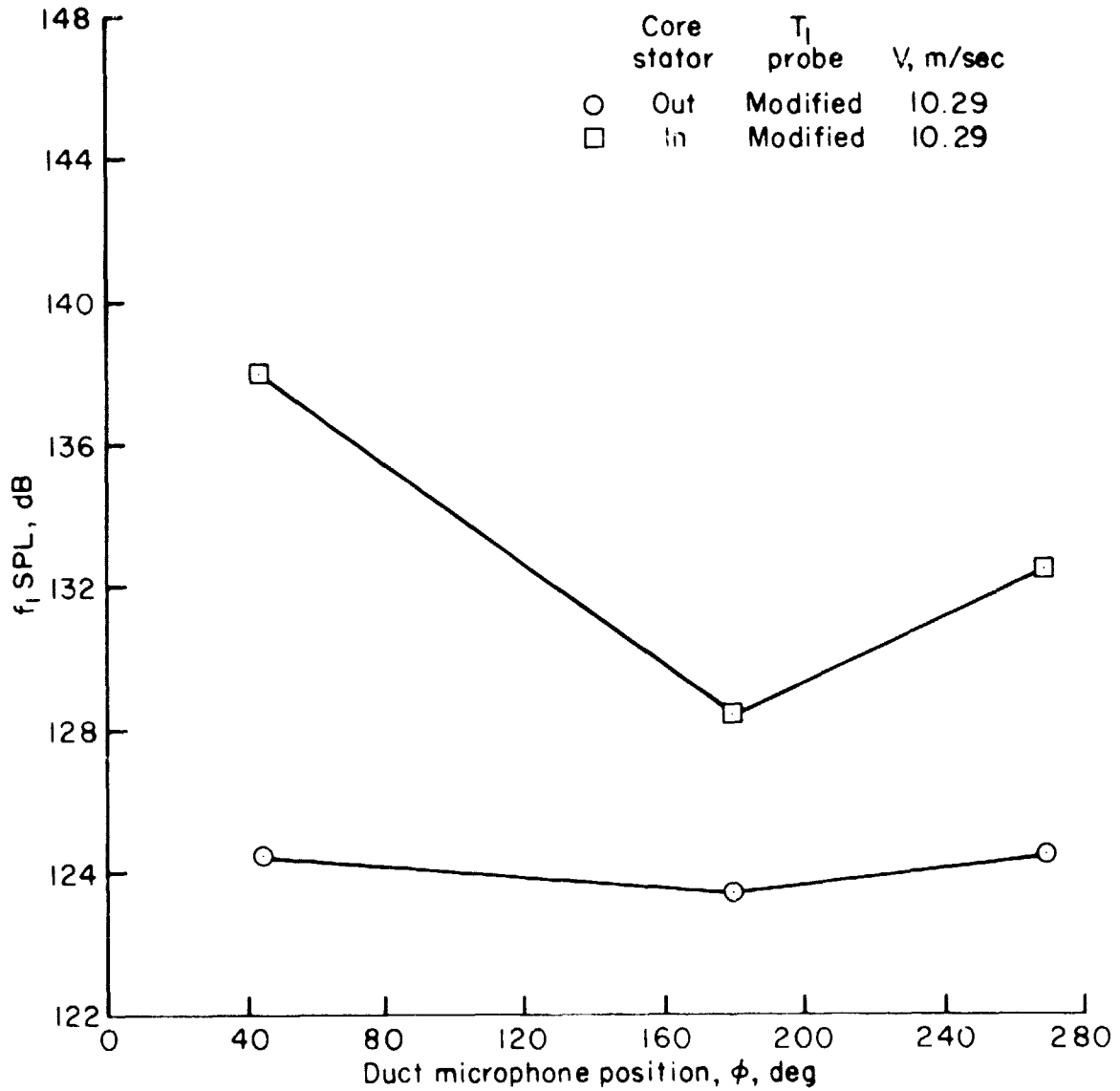


Figure 25.- Effect of core stator on in-duct  $f_1$  SPL at approach power with wind-tunnel simulation of forward speed: fan rpm<sub>n</sub> = 10,230; cruise inlet;  $\alpha = 0^\circ$ ; 40-sec sample.